RSC Advances

Cite this: *RSC Advances*, 2012, **2**, 12606–12623

www.rsc.org/advances

REVIEW

Structure and mechanical properties of beetle wings: a review

Jiyu Sun*[ab] and Bharat Bhushan*[b]

Received 25th June 2012, Accepted 27th September 2012
DOI: 10.1039/c2ra21276e

Insects of extremely small size have evolved to solve many problems. Their structure and mechanical properties information can be utilized to mimic them for industrial applications. Since beetle (Coleoptera, an order of insects) wings exhibit special functionalities, they have sparked worldwide research attention. Beetle wings are composed of a forewing (also known as elytron) and a hind wing. The elytra are rigid. A beetle's functional wings, which allow flying, are the hind wings. The elytra have an ingenious structure with superhydrophobic characteristics, a structural coloration and anti-adhesion characteristics. Their inner structure helps to provide light mass and high strength. The rotation angle and wing locking system of elytra are important features which increase beetles' ability to fly; they may furnish an insight for portable micro air vehicles (MAVs) and also provide inspiration for the design of bioinspired deployable systems. Studies of the structural and mechanical properties in biological systems may improve the understanding of natural solutions and advance the design of novel artificial materials. In this paper, the structure, mechanical properties and their relationship to function of beetle wings are discussed. Examples of bioinspired structures and materials are also presented.

1. Introduction

One of the greatest challenges for today's engineering science is miniaturization.[5,37] In this regard, insects of extremely small size have faced similar problems during their evolution.[6,99] Bioinspiration opens up new directions in materials science, nanotechnology, photonics and several other fields of science and technology.[4–7] Since the beetle (Coleoptera, an order of insect) is the most diverse insect order (comprising about 400 000 species) and exhibits some remarkable features, its wings have sparked worldwide research attention.[23]

Beetle wings are composed of a forewing (also known as elytron) and a hind wing; see Fig. 1. Most beetles have hardened

[a]*Key Laboratory of Bionic Engineering (Ministry of Education), Jilin University, Changchun, 130025, P. R. China. E-mail: sjy@jlu.edu.cn*
[b]*Nanoprobe Laboratory for Bio- & Nanotechnology and Biomimetics (NLB2), The Ohio State University, 201 W. 19th Avenue, Columbus, OH 43210-1142, USA. E-mail: bhushan.2@osu.edu*

Jiyu Sun

Prof. Jiyu Sun is an Associate Professor in the College of Biological and Agricultural Engineering and The Key Laboratory for Bionic Engineering, Jilin University, China.

Bharat Bhushan

Dr. Bharat Bhushan is an Ohio Eminent Scholar and The Howard D. Winbigler Professor in the College of Engineering, and the Director of the Nanoprobe Laboratory for Bio- & Nanotechnology and Biomimetics (NLB2) at the Ohio State University, Columbus, Ohio. His research interests include fundamental studies with a focus on scanning probe techniques in the interdisciplinary areas of bio/nanotribology, bio/nanomechanics and bio/nanomaterials characterization and applications to bio/nanotechnology, and biomimetics. He has authored 8 scientific books, 90+ handbook chapters, 800+ scientific papers (h index–57+; ISI Highly Cited in Materials Science, since 2007; ISI Top 5% Cited Authors for Journals in Chemistry since 2011), and 60+ scientific reports. He has also edited 50+ books and holds 17 U.S. and foreign patents.

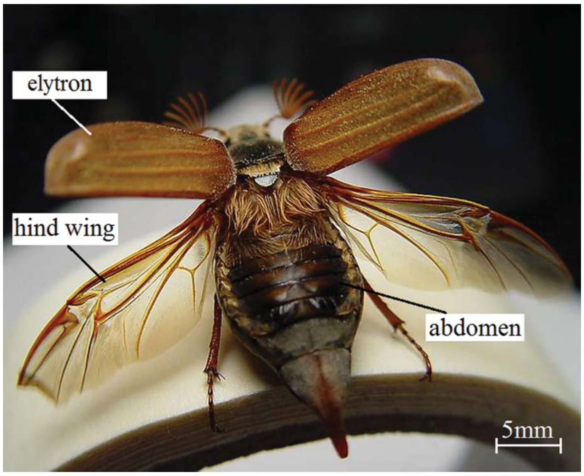

Fig. 1 Elytra and hind wings unfolding in a beetle, Cockchafer *Melolontha melolontha*.

elytra (some water beetles, such as Meloidae and Staphylinidae, have very soft elytra) which are not for flight, but serve to form a protective cover for the hind part of the body (the hind wings and abdomen). The hind wing is longer than the elytron, folded longitudinally and transversely under the elytron on the abdomen when at rest.[29] For flight, most beetles unfold their hind wings, and the elytra rotate and lift up. For Staphylinidae (a large group of ground-living beetles), because their elytra are very short, the hind wings quickly unfold from the elytra at takeoff. The opening/closing articulations of the elytra are complex in both structure and function.[37,119] The hind wing is thin and fragile, while the presence of resilin in the joints of the hind wings allows for repeated folding/unfolding action and keeps the wing in a folded position.[43,46,47] There are a few species of beetles without the second pair of wings as they usually live on the ground or within decaying plant material, such as the ground beetle (family Carabidae) and some "true weevils" (family Curculionidae).[53]

Elytra, as a natural biocomposite optimized by nature over many centuries, have excellent mechanical and physical properties, such as light weight, high strength, superhydrophobic characteristics, color changes and anti-adhesion characteristics. These are closely related to the microstructure both on the surface and inside. The unusual strength and toughness of insect cuticles, crustacean shells, mollusk nacre, and other chitin-containing living materials depend on complex structural interactions between chitin polysaccharides and proteins in these materials.[26]

Some special micro-structures have been found on the surface of elytra. The existence of longitudinal nodal grooves can help reduce drag resistance.[104] The wing scale arrays and grating microstructures allow beetles to display iridescent colors.[24,56,68,82,112] The color phases can also be created by "wax filaments" that spread from the tips of miniature tubercles that cover the cuticle surface.[49] The microtrichion arrays on the elytra increase the friction and help attach the wings to the body.[35,51,89,90]

There are cavities and preformed holes (pore canals and dermal glands) found in the elytra, which provide light mass and high strength coupled with excellent impact damage tolerance.[16,41] The reasons are that the inner microstructures including trabeculae, arrangement of chitin fibers, and helicoidal plies and continuous chitin fibers traveling around holes provide support and reduce the weight.

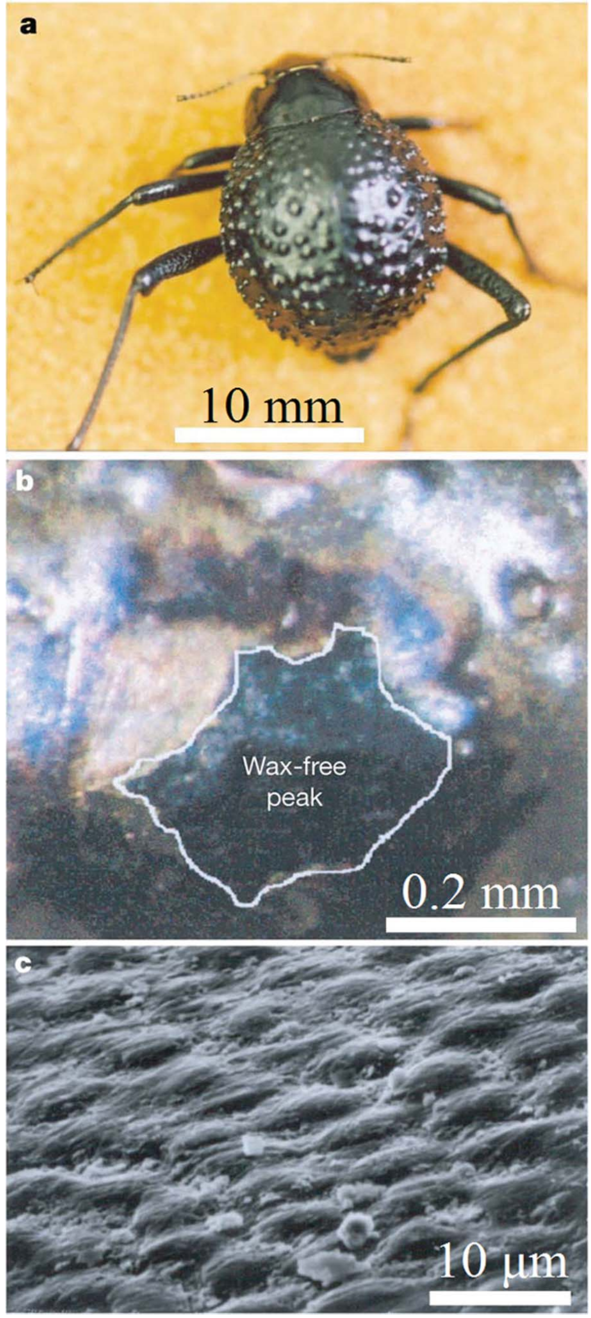

Fig. 2 The water-capturing surface of the fused elytra of the desert beetle *Stenocara sp.* (a) Adult female, dorsal view; peaks and troughs are evident on the surface of the elytra; (b) A 'bump' on the elytron; depressed areas of the otherwise black elytron are stained positively (waxy, colored), whereas the peaks of the bumps remain unstained (wax-free; black); (c) scanning electron microscopy (SEM) of the textured surface of the depressed areas.[80]

The wax coating on elytra provides beetles with superhydrophobic characteristics. One well known example is the Namib Desert beetle which can collect drinking water from fog-laden wind through the wax-free (hydrophilic) region found at the top of its bumps, while the troughs on the rest of the elytra surface have a hydrophobic character, as shown in Fig. 2.[80] This characteristic also helps dung beetles to reduce soil adhesion.[106] It has been reported that the texture of the wing surface can enhance its hydrophobicity,[84,87] but not all elytra with micro-scale features have hydrophobic characteristics.[10] Hydrophobic characteristics are also related with lifestyle habits and requirements for living activities.[58]

As for butterfly wings, there is a strikingly diverse array of iridescence mechanisms in beetles, and sometimes they are referred to as ''living jewels''. The color produced by these various optic mechanisms is sometimes termed ''structural color''.[93,96] The structural coloring of elytra has been speculated to help with camouflage, aposematic color, sexual signals and thermoregulation.[49,92,93,110] Some beetles' elytra colors change with the absorption of moisture as a result of variations in humidity, temperature and environmental conditions.[57,64,66,85,86,98,109]

The wing locking system of elytra and the folding/unfolding characteristics of hind wings are special features of beetles. Folding may sometimes occur along the flexion lines.[52] Wing venation and the distribution pattern of resilin will have an effect on folding patterns.[25,46,47,117,118] In general, wing extension probably results from the contraction of muscles attached to the basalar sclerite or, in some insects, to the subalar sclerite.[11] The folding/unfolding mechanisms of beetle hind wings may provide insights for the design of portable MAVs with morphing wings and give inspiration to develop bioinspired deployable systems.[3,6,48,101]

Studies of structural and mechanical properties in biological systems may deepen the understanding of natural solutions and advance the design of novel artificial materials.[22] From the tensile test, the mechanical properties of elytra appear to be related to the arrangement of a tough type of anisotropic chitin fibers.[13,19,55,67,101] However, it is difficult to measure their local mechanical properties, as they are highly structured biological composite materials with micro-scale thickness. The nanoindenter is useful to resolve this problem.[5,22,100,102–104] It enables the investigation of the local mechanical properties of beetle wings, which helps with understanding their natural design, heightens interest in the optimization of the biocomposites, and reveals their potential utility in materials science and engineering applications.

Organisms have survival mechanisms to cope with and adapt to their environment during the evolutionary process, which is helpful for humans.[124] For example, the *Stenocara* beetles gathering water from fog have been mimicked to fabricate bioinspired patterned films,[17,20,34,125] fog-catcher designs, applications to clear fog from airport runways and dehumidification equipment.[124]

In this paper, the structure, mechanical properties and relationship to function of beetle wings are discussed. Examples of bioinspired structure and materials are also introduced.

Table 1 Classification of some beetle which have been investigated for structure and mechanical properties

Suborder	Superfamily	Family	Topics studied[a]	References
Polyphaga	Scarabaeoidea	Cetoniidae	2, 3, 4, 7, 8	7,19,23,75,120
		Geotrupidae	5	30
		Lucanidae	2, 5, 8	12–14,30
		Passalidae	2, 8	40,41
		Scarabaeidae	1, 2, 3, 4, 5, 6, 7, 8	10,12–14,16,19,22,23,29,30,38,44,46,47,50,55,60,61,65,68–70,73,75,85,86,94,97,100–104,106,112,116,123
	Hydrophiloidea (water scavenger beetles)	Hydrophilidae	2, 3, 7	12,23,58
	Curculionoidea (weevil)	Coccinellidae	2, 4, 6, 8	31,32,52
		Curculionidae	1, 2, 4, 7	23,33,69,75
		Ithyceridae	2, 4	33,82
	Cantharoidea	Cantharidae	6	28
	Staphylinoidea	Silphidae	5	29,30
		Staphylinidae	6	43
	Histeroidea	Histeridae	5	29,30
	Buprestoidea	Buprestidae (jewel beetles)	2, 4, 5	1,29,30,75
	Tenebrionoidea	Meloidae	2, 4	75
		Tenebrionidae	1, 2, 3, 4, 5, 6, 7, 8	8,17,20,21,35,36,43,49,54,58,67,80,116,124,125
	Chrysomeloidea	Chrysomelidae	1, 3, 5	2,10,29,30
		Cerambycidae	1, 2, 3, 4, 5, 6, 8	29,30,33,43,66,68
	Cucujoidea	Coccinellidae	6	46
Adephaga	Caraboidea	Carabidae	2, 3, 4, 5, 6	28–30,63,75
		Pterostichinae	3	58
	Dytiscoidea	Dytiscidae	2, 3, 5, 7	19,29,30,58
		Gyrinidae	3	58

[a] 1 – morphology; 2 – elytra internal structure; 3 – wettability; 4 – structural color; 5 – wing locking; 6 – hind wing folding;7 – mechanical properties; 8 – biomimetic properties

2. Beetle species

With more than 350 000 species, beetles are the largest order of insects. The order includes four suborders, Polyphaga, Adephaga, Myxophaga and Archostemata (ordered from highest to lowest populated). The largest family, Curculionidae (the weevils, 17% of Coleoptera), contains around 50 000 described species, and the other large families Staphylinidae (13% of Coleoptera), Chrysomelidae (10% of Coleoptera), Scarabaeidae (8% of Coleoptera), Carabidae (8% of Coleoptera), Cerambycidae (6% of Coleoptera), Tenebrionidae (5% of Coleoptera) and Buprestidae (4% of Coleoptera) are all widespread terrestrial groups.[27,72]

Polyphagans include the vast majority of beetle diversity, with at least 300 000 described species from more than 100 families, or approximately 90% of the beetle species so far discovered.[18] They include furniture beetles, skin beetles, lady beetles, longhorn beetles, weevils, checkered beetles, leaf beetles, click beetles, fireflies, scarab beetles, stag beetles, rove beetles and water scavenger beetles.

Adephaga are also a diverse group, second in size only to Polyphaga, including 30 000 species in a dozen families and comprising about 10% of beetle diversity.[18] They include, among others, ground beetles, tiger beetles, whirligigs, predaceous diving beetles and wrinkled bark beetles. The family including the highest number of species is Carabidae, or ground beetles, with a predominantly predaceous feeding habit.[91] Many of Caraboidea are terrestrial, others are aquatic or semi-aquatic.[53]

Myxophaga is the second smallest suborder of Coleoptera after Archostemata, comprising families Lepiceridae, Torrincolidae, Hyddroscaphiidae, and Sphaeriusidae.[91] They are highly specialized for aquatic and semi-aquatic life, living amongst sand grains and other particulates and grazing on films of green and blue-green algae.[39]

Archostemata is the smallest suborder of beetles, comprising approximately 35 recent species, and is consistently shown as the

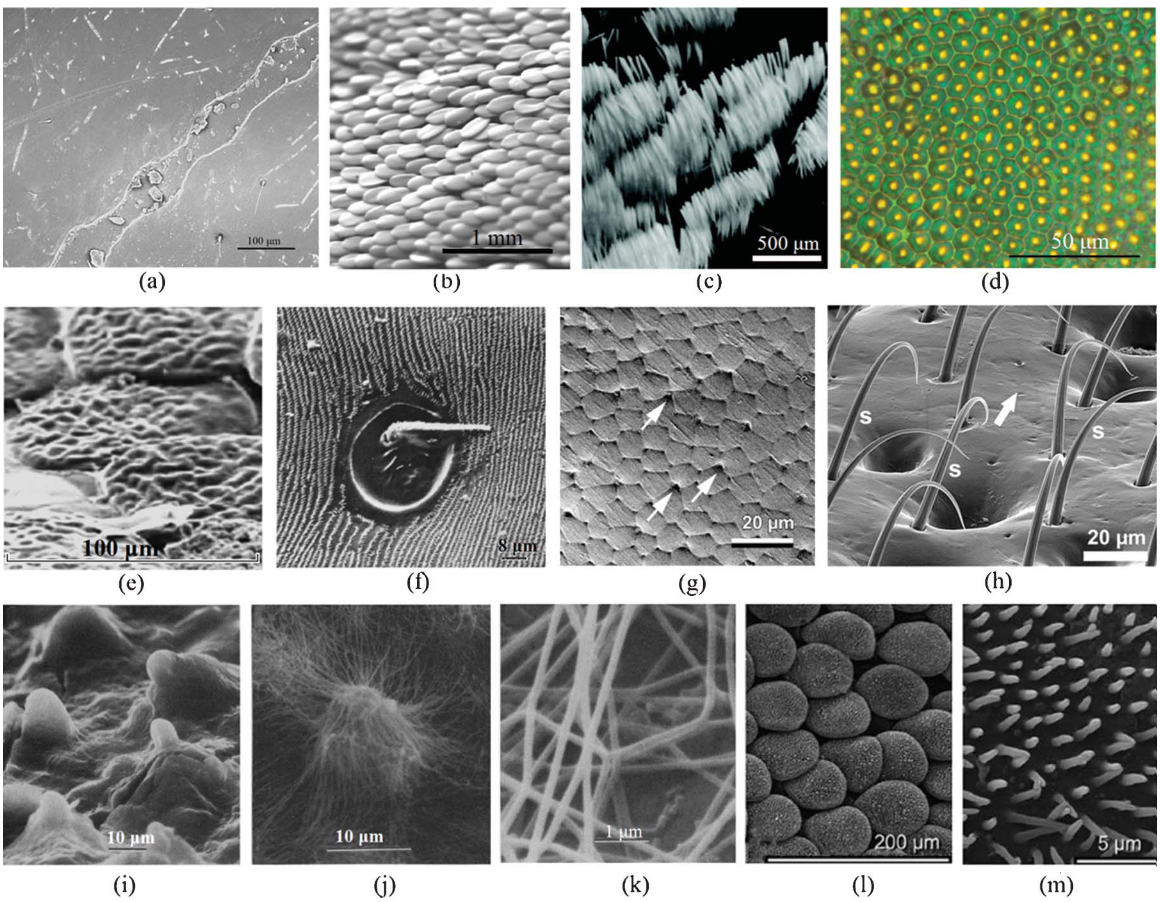

Fig. 3 Morphologies of beetle wings. (a) Field emission scanning electron microscopy (FESEM) of longitudinal node grooves and the channel in the nodes in the elytron of dung beetle, *Copris ochus* Motschulsky.[104] (b) and (c) Optical images showing the arrangement of white scales imbricating the elytra of *Cyphochilus* beetle[112] and *Calothyrza margaritifera*.[68] (d) Optical image of the elytra of beetle *Chrysina gloriosa*, showing bright yellow reflections from the core of each cell ($\sim$10 mm in size) and greenish reflection from the edges.[94] (e) SEM image of several partially overlapping green scales on the elytra of beetle *Pachyrrhynchus argus*.[82] (f) SEM image of diffraction grating of the elytra of the scarab beetle *Sericesthis geminata*.[56] (g) Cryo SEM image of the elytron surface in a fresh female *Leptinotarsa decemlineata*, hexagonal-shaped cells and small pores (arrows) are shown and grease smeared over the surface is visible.[111] (h) SEM image of elytral setae of *Galerucella nymphaea*.[2] (i) SEM image of miniature wax-secreting tubercles on the elytral surface of a black phase beetle (*Cryptoglossa verrucosa*).[49] (j) SEM image of wax filaments spreading from the tips of single tubercles in response to low humidity in a light blue phase beetle, and (k) high magnification of individual wax filaments (*Cryptoglossa verrucosa*).[49] (l) and (m) Scales on the dorsal surface and the surface of a single scale on the elytron of a scarabaeid beetle, *Hoplia sp*.[38]

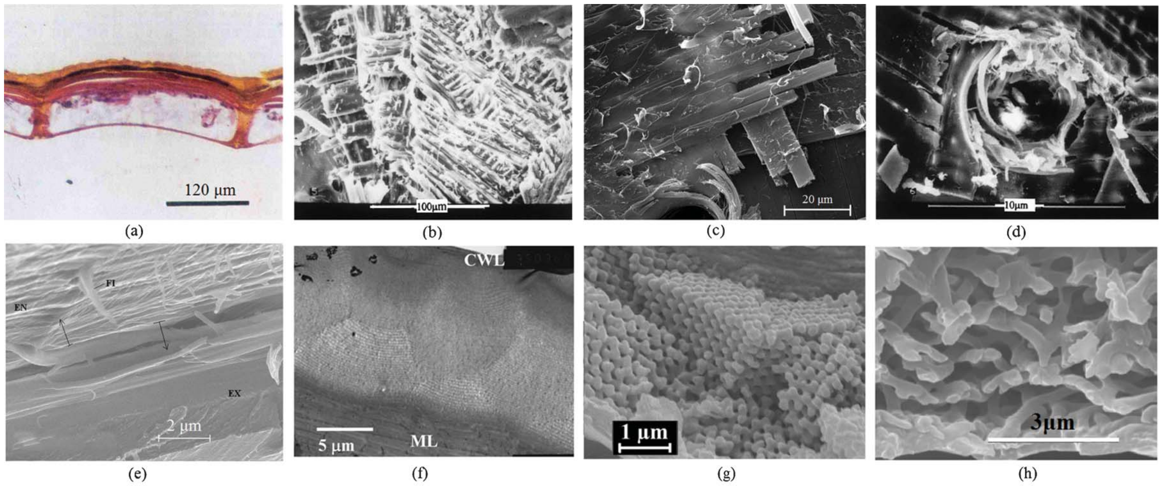

Fig. 4 Inner structures of beetle wings. (a) Transverse section of the elytron of a dung beetle (*Copris ochus* Motschulsky) showing the cavity and the pier-formed pillar structures within.[16] (b) Dual helicoidal arrangement of laminates of plies was found in the cuticle of a Hydrophilidae beetle. (c) The elytron of the carabid beetle (Carabusarcensis) is composed of long chitin fibers which cross in layers one above the other at 90° angles. Individual fibers are also interlinked with thin fibers which further enhance the coherence of individual layers.[63] (d) Hole used as a transport channel with chitin fibers surrounding it.[12] (e) FESEM image of the cross section of the elytron of a dung beetle (*Copris ochus* Motschulsky); EX, exocuticle; EN, endocuticle; FI, chitin fiber (many microfibrils are grouped together to form the fiber);[103] (f) TEM image collected from the cross-section of the elytron of a *P. boucardi* beetle, showing Bouligand planes highlighting the helicoidal nature of the layers of fibrous chitin, CWL, cuticular wax layer, ML, and melanin layer.[61] (g) SEM image of the cross-sectional view of the converting photonic scale of the internal photonic polycrystal structure of the elytron of a weevil *Pachyrrhynchus congestus pavonius* (Curculionidae).[114] (h) SEM image of the fractured edge of one of the white scales on the elytron of a *Cyphochilus* spp. beetle.[112]

most basal lineage in all studies on the relationships of beetles.[39] Myxophaga and Archostemata account for less than 1% of the living beetle diversity.[18]

Table 1 shows the classification of some beetle which have been investigated for structure and mechanical properties. The distributions of species investigated mostly belong to the family Scarabaeidae. *Allomyrina dichotoma* (Japanese rhinoceros beetle) and *Stenocara gracilipes* (Namib Desert beetle) have received much attention. But there are few investigations of Myxophaga and Archostemata at present.

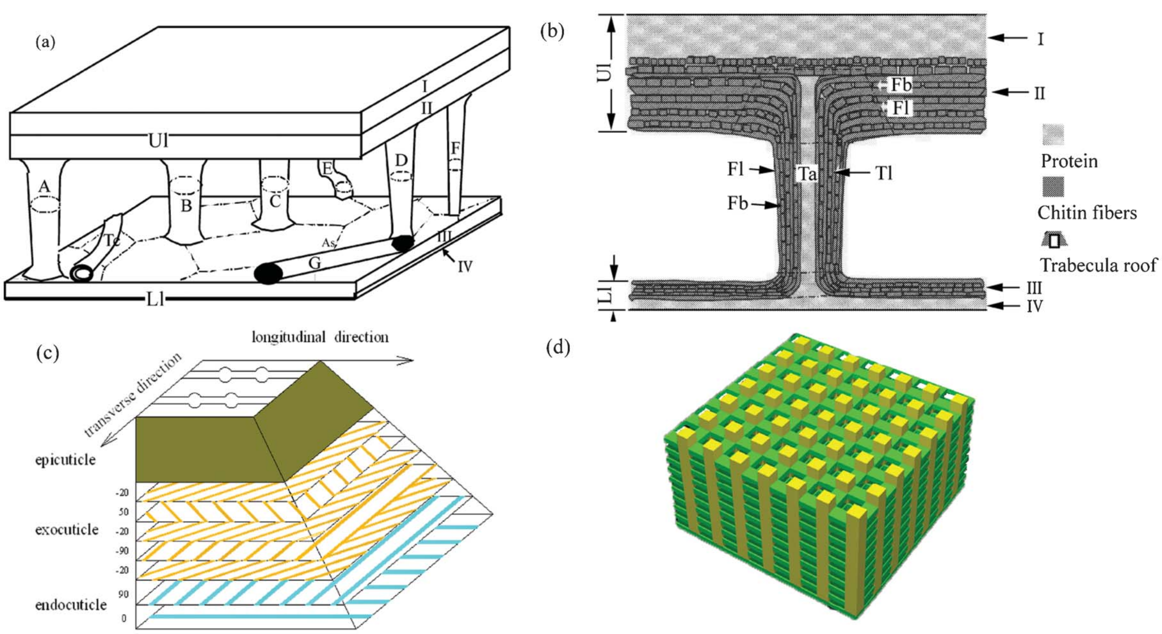

Fig. 5 Models of elytron structure. (a) and (b) Models of the trabecula of elytra.[60] (c) Fiber reinforced, hierarchically structured model of elytra.[103] (d) Model of the structure producing the color of the elytra of *Dynastes hercules.* The porous structure consists of chitin plies linked to each other by chitin chains.[85]

3. Wing structure and function

3.1 Surface morphology

There are some special micro-structures on beetle wings (Fig. 3), whose relationship with function will be discussed. There are longitudinal node grooves on the surface, and accumulated amounts of some substances are contained in the nodes of the dung beetle, *Copris ochus* Motschulsky (Fig. 3a). The arrangement of the wing scales favors the display of iridescent colors.[24] The whiteness of *Cyphochilus* spp. and *Calothyrza margaritifera* originates from the arrangement of white scales that imbricate above its elytra (Fig. 3b and 3c[68,112]). These scales are about 5 μm thick, 250 μm long and 100 μm wide.[112] *C. margaritifera* has a slightly different scale structure from *Cyphochilus* spp. It is typically 200–250 μm long but only 15 μm wide, resulting in a hairlike shape. In Lepidoptera and Psocoptera, scales provide color and pattern, which serve many functions in defense, display and thermoregulation.[118] In bright field microscopy, the structure of elytra of *Chrysina gloriosa* seems to consist of hexagonal cells (∼10 mm), where each cell appears to be green with a bright yellow core or nucleus (Fig. 3d).[94] This color derives from scales that are about 0.1 mm in diameter on the elytra of beetle *Pachyrrhynchus argus* (Fig. 3e[82]). Diffraction grating microstructures were found in the elytra of the scarab beetle *Sericesthis geminata* (Fig. 3f[56]). SEM of the elytron surface of a fresh female *Leptinotarsa decemlineata*, showed hexagonal-shaped cells with small pores (arrows) and visible grease smeared over the surface (Fig. 3g[111]). The body is completely covered with setae which render the tiny beetle *Galerucella nymphaea* water repellent (Fig. 3h[2]). Fig. 3i–3k shows SEM images of miniature wax-secreting tubercles on the elytron surface of a black phase beetle (*Cryptoglossa verrucosa*), wax filaments spreading from the tips of single tubercles in response to the low humidity in a light blue phase beetle, and high magnification of individual wax filaments.[49] Scales are found on the dorsal surface of the elytra of the scarabaeid beetle (*Hoplia sp.*) and on the surface of single scales (Fig. 3l and 3m[38]).

Additionally, cuticular scales on elytra, which should be wear-resistant, have been suggested to be responsible for maintaining thermal balance and generate sound.[38,88]

3.2 Inner micro-structure

The insect exoskeleton, or cuticle, is an excellent example of a natural, structural, fiber-reinforced, polymeric composite and consists of epicuticle, procuticle and epidermal cells. The procuticle is subdivided into the exocuticle and the endocuticle.[71] The procuticle consists primarily of chitin fibers embedded in a proteinaceous matrix and provides structural shape and mechanical stability.[41] As the procuticle forms, it is laid down in thin lamellae with chitin microfibers oriented at a slightly different angle in each subsequent layer.

The elytron's high structural strength and lightness is attributed to a honeycomb structure, trabecula, and stacked cuticle layers on microporous matrices.[13,60] Cavities are found on the elytra and they consist of two halves joined by a series of connectors, called trabeculae, which provide support and reduce weight[16,41] (Fig. 4a). Dual helicoidal forms of ply have been found in Hydrophilidae beetle cuticle as shown in Fig. 4b, which appears to depend on their location in the cuticle. The difference in angle between neighboring helicoidal plies is about 25°, and that between successive plies is about 85°. The same micro-structure has been found in the elytra of the carabid beetle (*Carabus arcensis*), which appears to be made up of a series of laminated laths consisting of smaller chitin fibrils embedded in a protein matrix. The fibrils are unidirectional within each ply and the plies are oriented at various angles (Fig. 4c). Many holes (or pore canals) in the cuticle have been reported (Fig. 4d); the chitin fibers go around these holes.[12] The epicuticle can be easily distinguished under the surface and wax layer, some of the chitin fibrils even connect to adjacent fibers creating a network of fibril bridging (upper half of Fig. 4e). TEM images collected from the

Table 2 Wetting characteristics of beetle wing surfaces

Species	Contact angle (°)^{a,b,c}	Habit	References
Agonum fuliginosum	102 (E, W)^1; 89 (E, W)^2	Terrestrial	58
Agonum obscurum	96 (E, W)^1; 80 (E, W)^2	Terrestrial	58
Agonum thoreyi	104 (E, W)^1; 89 (E, W)^2	Terrestrial	58
Agonum viduum	101 (E, W)^1; 84 (E, W)^2	Terrestrial	58
Allomyrina dichotoma	54 (E, W)^3	Terrestrial	10
Cetonischema aeruginosa	90 (E, W)^3	Terrestrial	120
Chrysolina virgata	71 (E, W)^3	Terrestrial	10
Chrysomela populi	30 (E, W)^3	Terrestrial	10
Copris ochus	91.5 (E, W)^3	Terrestrial	106
Dytiscus marginalis	90 (E, W)^1; 10 (E, W)^2	Aquatic	58
Galerucella nymphaea	159 (E, W)^3	Terrestrial	2
Gyrinus marinus	105 (E, W)^1; 90 (E, W)^2	Water surfaces	58
Hydrobius sp.	87 (E, W)^1; 0–50 (E, W)^2	Aquatic	58
Lagria hirta	81.7 (E, W)^3; 113 (H, W)^3	Terrestrial	116
Mimela testaceipes	68 (S, E, W)^3	Terrestrial	10
Onymacris bicolor and *Onymacris unguicularis*	>90 (E, W)^3	Terrestrial	54
Pachnoda marginata	31.6 (E, W)^3; 82.2 (H, W)^3	Terrestrial	116
Tenebrio molitor	107 (E, W)^1; 92 (E, W)^2	Terrestrial	58
Tmesisternus isabellae	29.2, 105.7 (E, W)^3	Terrestrial	66
Zophobas morio	43.0 (E, W)^3; 86.3 (H, W)^3	Terrestrial	116

^{a} ^{1} advancing angle; ^{2} receding angle; ^{3} static contact angle. ^{b} Segment: E, elytra; H, hind wing; S, Setae. ^{c} Test solution: W, Distilled or deionized water.

Table 3 Relationships between structural colors, microstructure and optical mechanisms in beetles

Structural color		Microstructure[a]	Optical mechanism	References
Simple metallic hues	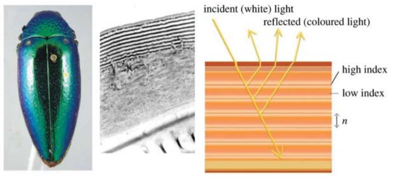	Curved multilayers[I]	Multilayer reflection	93,97
Circularly polarized colour	Fig. 3d, Fig. 4f 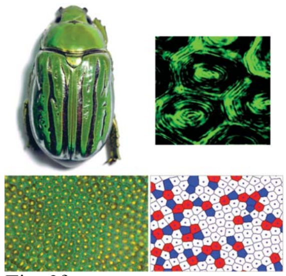	Hexagonal array[M]	Helically arranged multilayer reflection	61,94
Iridescence	Fig. 3f 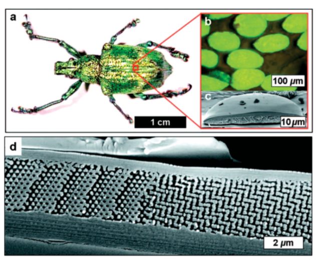	Grating[M] ; photonic diamond-based crystal lattice[S]	Diffraction grating	31,32,56
Opal or diamond effects	Fig. 3e 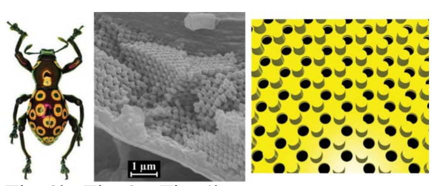	Transparent spheres array[S]	Three-dimensional photonic crystal	82,114
White	Fig. 3b, Fig. 3c, Fig. 4h 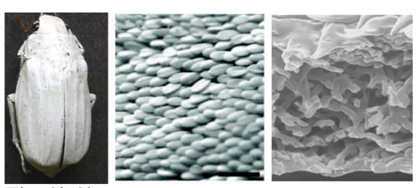	Packed nanofilaments[S]	Tyndall scattering	68,79,112
Color changing	Fig. 3i–3k 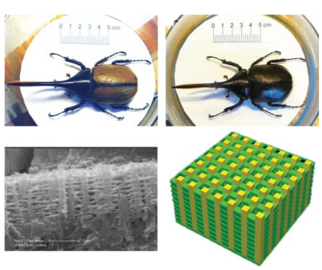	Porous structure[S]; wax filament[M]	Heat or humidity sensitivity	1,49,85

[a] M, microstructure of elytra; I, internal microstructure of elytra; S, internal microstructure of scales.

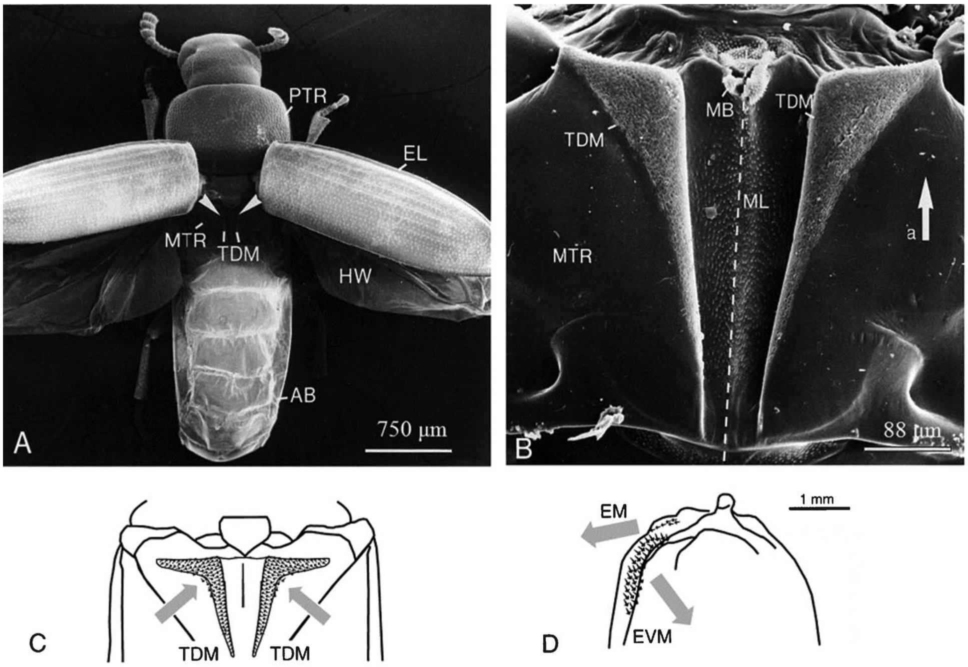

Fig. 6 Wing-locking system of *Tribolium castaneum*, TDM microtrichial fields. SEM images of (a) locations of TDM microtrichial fields and (b) dental-wax-cast filled with spur resin. (c) Directionality of microtrichia in the thoracic dorso-medial field. (d) Directionality of microtrichia in the elytra fields. AB, abdomen; EL, elytra; HW, hind-wing; MB, membrane; ML, midline; MTR, metathorax; PTR, prothorax; TDM, dorso-medial field of the thorax. EM, medial field of the elytra; EVM, ventro-medial field of the elytra.[36]

cross-section region between the cuticular wax layer and the melanin layer of the elytra of the *P. boucardi* beetle show a distinct structure in the form of shallow, concentrically arced layers below the surface with a diameter of about 8 µm (Fig. 4f). They correspond closely to the diameter of the hexagons observed under optical microscopy (Fig. 3d).[61] The SEM view shows the internal structure of the converting photonic scale of the weevil *Pachyrrhynchus congestus pavonius* (Curculionidae), which resembles a crystal lattice (Fig. 4g).[114] The layered structure is apparent, but very regular fractures in the direction roughly normal to the layers indicate a highly correlated stacking of these layers in accordance with their biopolymeric photonic properties.[31,32,114] For the white scales on the elytron of a *Cyphochilus spp.* beetle, the SEM image shows that the fractured edge is composed of a random network of interconnecting cuticular filaments with diameters of about 250 nm (Fig. 4h).[112]

According to the microstructure of elytron cuticles observed in transverse and longitudinal directions, a model was proposed as shown in Fig. 5. Fig. 5a and 5b show the models of the trabecula of elytra;[60] Fig. 5c illustrates the chitin fiber reinforced, hierarchically structured model of elytra;[103] and Fig. 5d shows a porous structure model consisting of chitin plies linked to each other by chitin chains which produce the color of the elytra of *Dynastes hercules*.[85]

3.3 Wettability properties

Some beetles in the Namib Desert collect drinking water from fog-laden wind through their hydrophobically–hydrophilically structured back, which exhibits dynamic anisotropic wetting properties with the ability to collect or repel water to assist the beetle with its daily tasks (Fig. 2[80]). On a macroscopic scale, a near-random array of bumps (0.5 mm in diameter) covers the elytra (Fig. 2a); at the microscopic level, the peaks of these bumps with no covering contrast the troughs covered by a wax coating (Fig. 2b). The microstructure of the wax coating consists of flattened hemispheres (10 mm diameter) arranged in regular hexagonal arrays (Fig. 2c), creating a superhydrophobic system reminiscent of the lotus leaf. As droplets grow to a critical size, they slide off of their unstable position at the peak of each bump and into the hydrophobic troughs where they can roll down towards the mouth of the beetle. A hydrophobic elytron surface is also observed in dung beetles, who break up and compact dung into balls with neither dung nor dirt sticking to their body or legs.[106] The 'non-smooth' morphologies found on the elytra (Fig. 3a and 3h) of many soil-burrowing beetles have also been shown to be self-cleaning, providing lower adhesion with soil, but in a totally different way from the desert beetle.[87]

In order to identify the wettability properties of beetle wings, their contact angles (CA) were investigated. Representative data are presented in Table 2. The CA on the hind wings (82.2°–86.3°) are significantly larger than those on the elytra (31.6°–43.0°) in *Lagria hirta* L., *Pachnoda marginata* and *Zophobas morio*.[116] The contact angle of the surfaces is above 90°, if an elevated roughness is observed on the cuticle surface.[74] The texture of the wing surface can enhance its hydrophobicity and enable droplets of water to roll off the wing and remove dirt.[6] But not all beetle wings with micro-scale features have hydrophobic characteristics.[10] The hydrophobic characteristics are also related with life habits and requirements of living activities.[58] Due to color changing needs, each elytron of the beetle *Tmesisternus isabellae* displays both hydrophilic or hydrophobic characteristics, with the colored band regions displaying hydrophilic characteristics

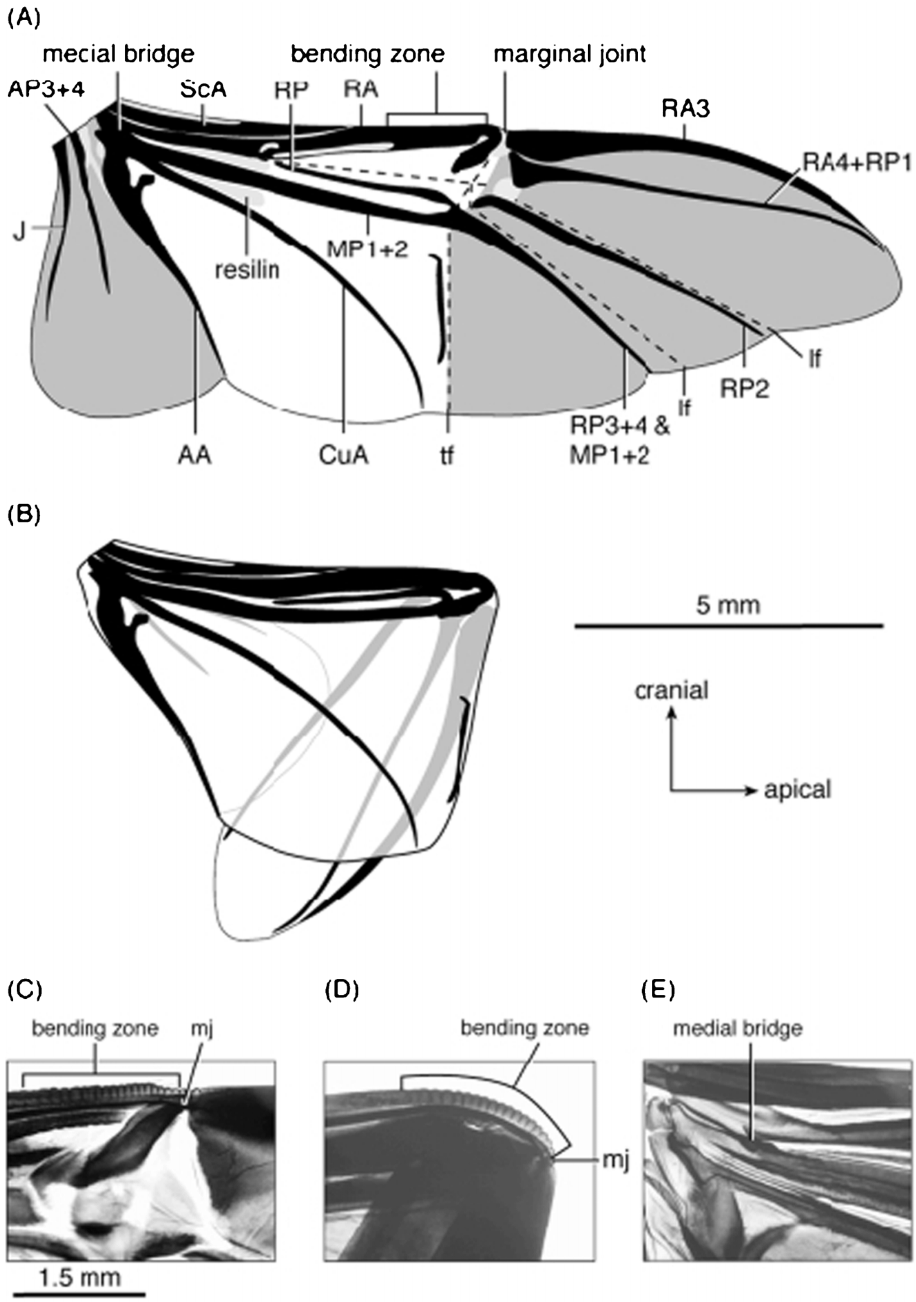

Fig. 7 Right hind wing of *Pachnoda marginata*, (a) unfolded and (b) folded. (c) and (d) The anterior wing margin is curved at the bending zone and sharply bent at the marginal joint when folded. The pivot of the scissors-like movement of RA and MP1+2 is the medial bridge (e, in the unfolded wing). Light grey shading indicates resilin in the wing; dark grey shading delimits apical and anal fields. AA, Analis Anterior; AP, Analis Posterior; CuA, Cubitus Anterior; J, Jugal; lf, longitudinal fold; MP, Media Posterior; RA, Radius Anterior; RP, Radius Posterior; ScA, Subcosta Anterior; tf, transverse fold.[44]

and the black band regions displaying hydrophobic characteristics, with CAs of 29.2° and 150.7°, respectively.[66] The hydrophilic parts can absorb humidity, which induces color changing. For beetles living surrounded by dirt, such as the dung beetle, the CA is above 90°.

3.4 Structural coloring

Beetles come in various different colors with a metallic shine, such as gold (*Chrysina resplendens*, *Aspidomorpha tecta*), silver (*Chrysina batesi*, *Chrysina strasseni*), gray (*Chrysina limbata*), blue (*Eupholus schoenherri petiti*), red (*Plusiotis chrysargirea*), and purple (*Smaragdesthes Africana oertzeni*, *Chrysina purulhensis*), which justifies the expression "living jewelry" sometimes used to refer to them.[24] Beetles develop their peculiar tints, sometimes referred to as "structural colors", through a microstructure with dimensions comparable or shorter than the wavelength of light.[96]

The origins of structural colors include microstructural morphology of the surface (Fig. 3b–3f) and inside of scales

Table 4 Mechanical properties of beetle wings

Segment	Species	Elastic modulus (GPa)[a,b,c]	Hardness (GPa)[a,b,c]	Tensile strength (GPa)[a,b,c]	Fracture toughness (MPa $\sqrt{m}$)[a,b,c]	References
Elytra	*Allomyrina dichotoma*	4.34 (D, V)[2]	0.15 (D, V)[2]			19
				0.13 (D, L)[1]		13
	Copris ochus Motschulsky	1.01–6.17 (D, V)[2]; 0.52–7.34 (D, T)[2]; 1.46–6.05 (D, L)[2]; 14.56 (F, L)[1]	0.09–0.33 (D, V)[2]; 0.03–1.66 (D, T)[2]; 0.09–0.84 (D, L)[2]	1.2 (F, L)[1]	1.56(D, V)[2]	100–104
	Cybister japonicus	1.19 (F, T)[1]; 1.41 (F, L)[1]; 0.56 (D, T)[1]; 0.59 (D, L)[1]; 5.1 (D, V)[2]	0.19 (D, V)[2]	0.17 (F, T)[1]; 0.19 (F, L)[1]; 0.09 (D, T)[1]; 0.09 (D, L)[1];		19
	Pachynoda sinuata	0.09–2.46 (F)[1]		0.04–0.11 (F)[1]		55
	Potosia brevitarsis	5.45 (D, V)[2]	0.24 (D, V)[2]			19
	Serrognothus titanus	8.16 (D, V)[2]	0.48 (D, V)[2]			19
	Tenebrio molitor	0.05 (UT, L)[1]; 0.32 (PT, L)[1]; 1.0 (FT, L)[1]; 2.3 (D, L)[1]; 0.04–0.05(UT, L)[3]; 0.44–0.54 (PT, L)[3]; 1.02–1.10 (FT, L)[3]; 0.03–2.20 (D, L)[3]		0.006 (UT, L)[1]; 0.01 (PT, L)[1]; 0.03 (FT, L)[1]; 0.007 (D, L)[1]	0.3 (UT, L)[1]; 0.4 (PT, L)[1]; 0.5 (FT, L)[1]; 1.0 (D, L)[1]	67
	Tribolium castaneum	0.04 (UT, L)[1]; 0.21 (PT, L)[1]; 0.03–0.06 (UT, L)[3]; 0.14–0.24 (PT, L)[3]; 1.2–1.3 (FT, L)[3]; 0.88–4.20 (D, L)[3]		0.004 (UT, L)[1]; 0.006–0.01 (PT, L)[1]	0.2 (UT, L)[1]; 0.4 (PT, L)[1]	67
		0.08 (UT, L)[4];				21
Hind wing	*Allomyrina dichotoma*	2.06–2.74 (D, C)[1]; 0.51–0.95 (D, S)[1]		0.02–0.05 (D, C)[1]; 0.005–0.02 (D, S)[1]		62
		2.97–4.5 (F, C)[1]; 1.63–2.24 (F, S)[1]				42

[a] Loading direction: V, vertical direction; T, transverse direction; L, longitudinal direction; C, chordwise direction; S, spanwise direction. [b] Testing methods: [1] Tensile; [2] Nanoindentation; [3] Dynamic experiments; [4] Transient mechanical testing. [c] Sample status: D, dry; F, fresh; UT, untanned; PT, partially tanned; FT, fully tanned.

(Fig. 4f–4h), and their interactions. For scaleless beetles, surface microstructure elements such as grating,[56] hexagonal array,[61,94] and wax filaments[49] are the main cause of selective metallic reflection. Scale bearing beetles exhibit diverse styles of internal microstructure, such as curved multilayers,[97] crystal lattice,[31] transparent spherical array,[82,113] nanofilaments,[68,79,112] porous structure,[1,85] and a thin flat slab with parallel rods.[86] From the point of view of the optical mechanism, the iridescence mechanisms observed in beetles can mainly be classified into three mechanistic groups: multilayer reflectors, three-dimensional photonic crystals, and diffraction gratings.[93] The relationships between structural color, microstructure and optical mechanism are listed in Table 3.[93] The microstructures of elytra affect the structural color and optical mechanism. For example, due to stacked chitin layers (optically active or not) present in all beetles, multilayer reflectors are the most widespread iridescence mechanism.[93]

The structural colors of elytra are actually interference colors mixing partly to produce camouflage by matching the color of the environment.[92] For tiger beetles, bright iridescent coloration (aposematic color), implicated in predator evasion during flight, was part of a defensive strategy usually acting in combination with chemical defenses.[110] The metallic colors also play a role in sexual signaling.[93]

Changes in the level of hydration cause a variation in the thickness of the multilayer stack, leading to a color change in elytra in accordance with predictions.[57,66,85,98,109] For a Hercules beetle in the dry state, nanosized holes in the layer are occupied with air (refractive index 1) but the empty holes are filled with water (refractive index 1.33) under high humidity, which induces a variation in the visible color.[64] The blue scales on the cuticle of the male beetle *Hoplia coerulea* can absorb water, with the consequence that these scales, which have been shown to be responsible for the beetle's bright blue coloration, reversibly turn to emerald green with increasing water content.[86] It is desirable for beetles to change color reversibly and rapidly for species and sex recognition, and also for camouflage and mimicry.[38] For the desert beetle *Cryptoglossa verrucosa* (LeConte), which changes color with humidity, the "wax filaments" meshwork that accumulates at low humidity reduces transcuticular water loss and may lower the rate at which the body temperature rises under a radiation load by increasing reflectance (Fig. 3i–3k[49]).

3.5 Wing locking system

In beetles, the system responsible for the attachment of elytron to thorax is composed of a few interlocking structures, located between thorax and abdomen, and between the left and right elytra (Fig. 6[35–37]). Beetle wings are attached to their body

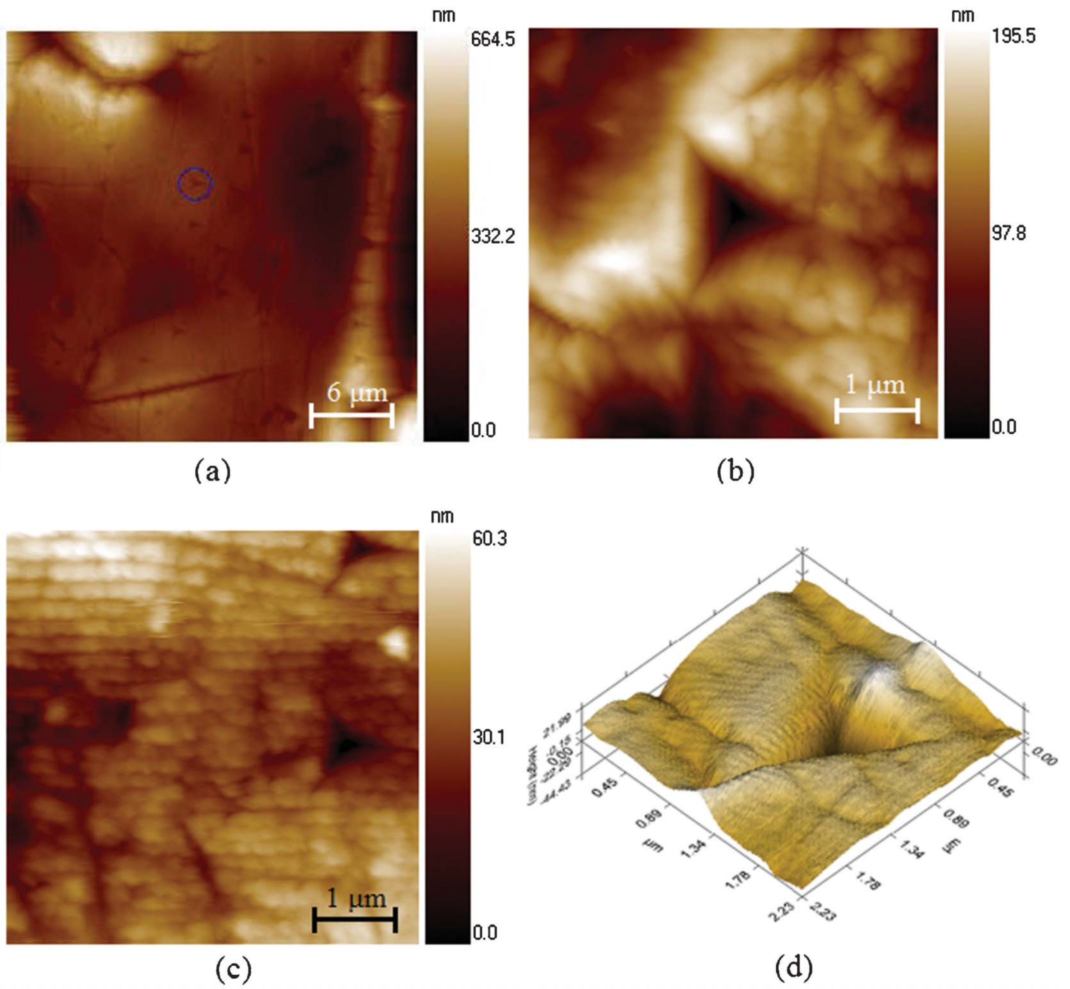

Fig. 8 *in situ* scanning images of the dry elytra after the test in (a) the vertical direction (the circle shows one indent), (b) the transverse direction, and (c) the longitudinal direction. One nanoindentation image (d) shows signs of the residual deformation and elastic recovery.[103]

through arrays of microtrichia (Fig. 3h), which are usually oriented in one preferred direction on the cuticular surface forming numerous hair-to-hair contacts to maximize lateral shear adhesion.[8,35,51,89,90] With regard to wing opening and closing, the double rotation of the elytron has one degree of freedom and the elytron to body articulation in beetles is a spherical mechanism with two separate but linked drives for a broad swing during opening or closing.[29,30]

3.6 Folding/unfolding characteristics

Forbes[28] first discussed beetle hind wings' folding. When at rest, the wings are held over the back in most beetles, which may involve longitudinal folding of the wing membrane and sometimes also transverse folding. Folding may sometimes occur along the flexion lines.[52] Though fold lines may be transverse, as in the hind wings of beetles, they are normally radial to the base of the wing, allowing inward retraction of the wing tip and adjacent sections of a wing to be folded over or under each other, as shown in Fig. 7.[9,44]

The functioning of the hind wing of a beetle involves a combination of several basic mechanisms, consisting of four plates connected by hinges.[45] The system possesses a single kinematic degree of freedom.[48] Some of the flexion lines are active not only in folding the wing away after flight, but also during the stroke, where they play a dynamic role in altering wing profile. Wing venation will also affect folding patterns.[25,117,118] In general, wing extension probably results from the contraction of muscles attached to the basalar sclerite or, in some insects, to the subalar sclerite.[11]

The presence of resilin, a rubber-like protein, in some mobile joints has multiple functions: the distribution pattern of resilin in the wing correlates with the particular folding pattern of the wing, resilin is found at the places where extra elasticity is needed, and it provides the wing with elasticity in order to be deformable by aerodynamic forces, which may result in elastic energy storage in the wing.[46,47]

4. Mechanical properties

4.1 Tensile properties

Depending on the orientation of the chitin fibers, the elastic modulus (E) of the elytron cuticle of the Rose chafer beetle, *Pachynoda sinuata*, varies from 0.9 to 2.42 GPa.[55] It appears that elytron cuticle design is based on attaining reasonable functional

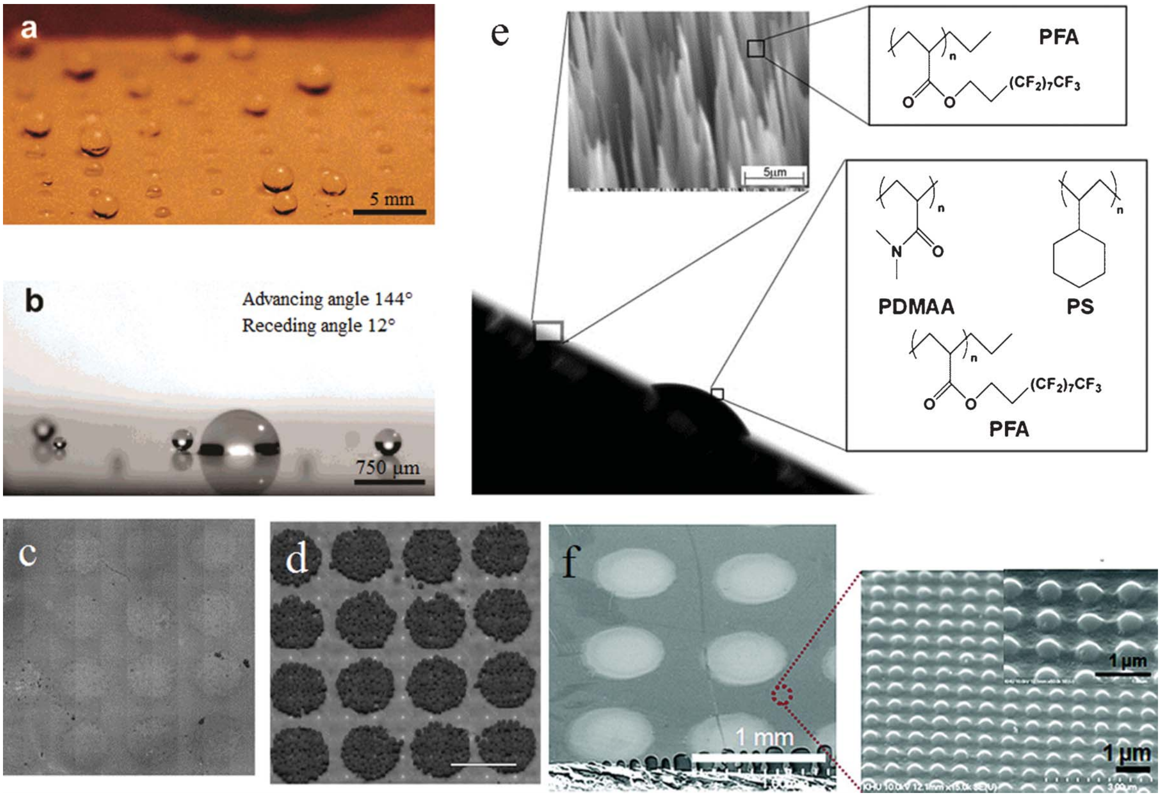

Fig. 9 Fog capture surfaces. (a) Small water droplets sprayed on a (PAA/PAH/silica nanoparticle/semi-fluorosilane) superhydrophobic surface with an array of hydrophilic domains patterned with a 1% PAA water–2- propanol solution, and (b) sprayed small water droplets accumulated on the patterned hydrophilic area shown in (a).[125] (c) Pulsed plasmadeposited poly(glycidyl methacrylate) array onto a CF_4 plasmafluorinated poly(butadiene) surface; (d) the same pattern reacted with 50 μm amino-polystyrene microspheres. The spots of pulsed plasma-deposited poly(glycidyl methacrylate) are 500 μm in diameter and 1 mm center-to-center.[34] (e) Side view micrograph of an artificial *Stenocara* beetle's back with hydrophilic bumps and hydrophobic background material. Insets show an electron microscopy image of the nanograss structure and the chemical formulas of the polymers that were used for coating the nanograss structure and for constructing bumps.[20] (f) FESEM of the SiO_2 hydrophilic dot pattern (~500 μm diameter) on a hydrophobic nanopatterned UV-cured resin surface, and a magnified AFM and SEM image of an imprinted hydrophobic surface (~400 nm in width, ~200 nm in depth, and ~700 nm center-to-center).[17]

isotropy from an inherently tough anisotropic fibrous structure. The mechanical properties of beetle wings are shown in Table 4.

Compared with the elytron, the value of the membrane of a beetle's hind wing is lower; *E* varies over the area of the wing and ranges from 2.97 to 4.5 GPa in the chordwise direction and from 1.63 to 2.24 GPa in the spanwise direction.[42] Furthermore, Poisson's ratio in the chordwise direction is 0.63–0.73 and approximately twice as large as that in the spanwise direction (0.33–0.39), and it can be concluded that the membrane of a beetle's hind wing is an anisotropic and non-homogeneous material.

To investigate the cross-linking relationships between components, the hydration and mechanical properties of the elytra of the beetles *Tribolium castaneum* (red flour beetle) and *Tenebrio molitor* (yellow mealworm) at various tanning stages were tested under static and dynamic conditions.[67] With increasing tanning, the elytron of *Tenebrio* changes from ductile and soft (E = 44 MPa) to brittle and stiff (E = 2400 MPa); the dynamic elastic moduli (E') increase by nearly 20-fold, whereas the frequency dependence of E' diminishes. These results support the hypothesis that cuticle tanning involves cross-linking of components, while drying to minimize plasticization has a lesser impact on cuticular stiffening and frequency dependence.

For hind wings, both veins and membranes consist of a double layer of cuticle, a biological fibrous composite material with mechanical properties ranging from very stiff to flexible depending on its chemical composition.[46] *E* differed in relation to the membrane arrangement showing a structural anisotropy; in the chordwise direction, *E* is approximately 2.65 GPa, which is three times larger than *E* in the spanwise direction (0.84 GPa).[62]

4.2 Nanoindentation

Nanoindentation has become a useful tool for characterizing the mechanical properties of thin elastic and viscoelastic materials with low contact stiffness and manifold surface structures.[5,6,22] Tests on fresh and dried samples of dung beetle (*Geotrupes stercorarius*) using a nanoindenter show the influence of desiccation on the results and point out the importance of native conditions during the measurements.[22]

The nanomechanical properties of multilayer elytron cuticle of dung beetle (*Copris ochus* Motschulsky) were investigated in the vertical and transverse directions using a nanoindenter.[104] The E_v and hardness (H_v) values for the surface cuticle in the vertical direction obtained by nanoindentation were 3.54 GPa and 0.20 GPa, respectively. The nanoindentation result showed that the

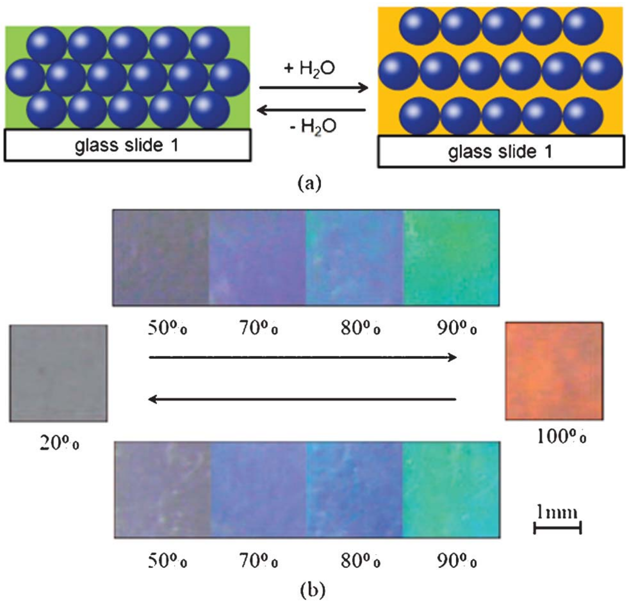

Fig. 10 Reversible changes of the color/stopband of the PAAm–P(St–MMA–AA) PC hydrogel with relative humidity. (a) The schematic illustration of the periodic structure change of a PC hydrogel before and after being fully wetted in water. (b) Photographs of the as-prepared PC hydrogel corresponding to different humidity. Photographs of the as-prepared PC hydrogel corresponding to relative humidities of 20%, 50%, 70%, 80%, 90% and 100%, respectively.[105]

modulus (E_t) and hardness (H_t) of each layer were gradually reduced from the outer layer to the inner layer in the transverse direction. E_v was less than the largest E_t obtained for the outer layer (7.06 GPa). This may be a result of the composite effect of the multilayer. The elytra belonging to beetles of other species were measured using a nanoindenter; E and H values ranged from 0.15–0.48 GPa and 4.34–8.16 GPa, respectively.[19]

Fig. 8 shows the *in situ* imaging of nanoindentation and surface morphology of a dung beetle's elytron in the vertical (Fig. 8a), transverse (Fig. 8b) and longitudinal direction (Fig. 8c), and one indent image in 3D view (Fig. 8d).[103] It can be observed that in the structure of the endocuticle, which is the larger layer in Fig. 4e, chitin fibers in the deeper layers are oriented in a direction nearly parallel to the surface of the endocuticle (Fig. 8c). The obtained modulus in vertical direction E_v and hardness H_v of the elytron cuticle were 5.96 $\pm$ 0.32GPa and 0.32 $\pm$ 0.09GPa, respectively.

5. Bioinspired structures

Polymers are ideal for forming a surface which will reproduce the *Stenocara* beetle's ability to gather water from fog. Depending upon the scale of the features required, different printing methods can be used to generate the features by depositing a second material, or the polymer can be modified to render it hydrophilic in patches (Fig. 9).[95] To mimick the back of the Namib Desert beetle, a method for printing superhydrophilic patterns on a superhydrophobic surface *via* a PAH/PAA/silica nanoparticles alternate deposition technique has been developed (Fig. 9a and 9b).[125] Hydrophilic patterns on superhydrophobic surfaces were created with water–2-propanol solutions of a polyelectrolyte to produce surfaces with extreme hydrophobic contrast. Selective deposition of multilayer films onto the hydrophilic patterns introduces different properties to the area including superhydrophilicity. Also, inspired by the design of the elytron surface of this beetle, different methods can be used to fabricate alternative superhydrophobic and superhydrophilic patterns on the surface,[122] such as pulsed plasma deposition,[34] micromachining,[20] and nanoimprinting.[17] Similar water collection structures were implemented on the surfaces of a series of superhydrophobic/hydrophilic patterns by employing a micro-condensation process using plasma chemical patterns.[34] It was found that water-collecting capabilities would occur in correspondence with a variety of superhydrophilic spot size and pattern ratios (Fig. 9c and 9d). A series of superhydrophobic surfaces with patterns with smooth circular hydrophilic domains were fabricated. It was found that the water collection efficiency could be optimized by controlling the wettability contrast of the superhydrophobic/hydrophilic patterns as well as the ratio of the pattern areas (Fig. 9e).[20] The results also indicated that the pinning force for a given bump was constant and did not depend on the drop volume. A transparent polymeric gas barrier nanopatterned surface was fabricated using UV-curable nanoimprinting techniques (Fig. 9f).[17] Potential applications of such surfaces include water harvesting surfaces, controlled drug release coatings, open-air microchannel devices, and lab-on-chip devices.[125]

The mimicking of the elytra of the desert beetle can be used for other potential applications such as to clear fog from airport runways and improve dehumidification equipment.[124] The superhydrophobic morphology of the surface of the elytra of the dung beetle has been used in the design and development of new mould boards for ploughs and new bulldozing plates to obtain reduced resistance and adhesion with soil, which have resulted in significant fuel savings.[87]

Since material properties are structure-dependent, new and interesting properties are expected from unusual or complex structures.[24] To mimick the multilayered structures of beetle wings, a biomimetic approach was used to fabricate thermally stable porous films by a layer-by-layer (LbL) self-assembly method.[121] Inspired by the preformed holes of elytra, forming the holes *in situ* during the processing phase of the composite allows the chitin fibers to remain continuous around the hole, which improved the strength and damage tolerance of the composites.[40,41] To develop lightweight composite structures that mimick the beetle elytron structures (such as honeycomb cores, trabeculae and an edge frame), a biomimetic manufacturing process was used to achieve integrated honeycomb plates with edge sealing.[15] Potential applications of dung beetle surface geometry include agricultural equipment such as furrow openers, plows and tillers which demonstrate lower resistance and power requirements against soil.[107,108]

Beetle elytra frequently exhibit fascinating coloration and some may even be switchable. Such nanoarchitectures have been successfully produced.[7,81,83] The multilayer structure found in the elytra of Taiwanese *Trigonophorus rothschildi varians* beetles exhibits a random distribution of cylindrical holes normal to the plane of the multilayer structure, and bioinspired artificial surfaces with similar properties show that such photonic nanoarchitectures of biological origin may constitute valuable

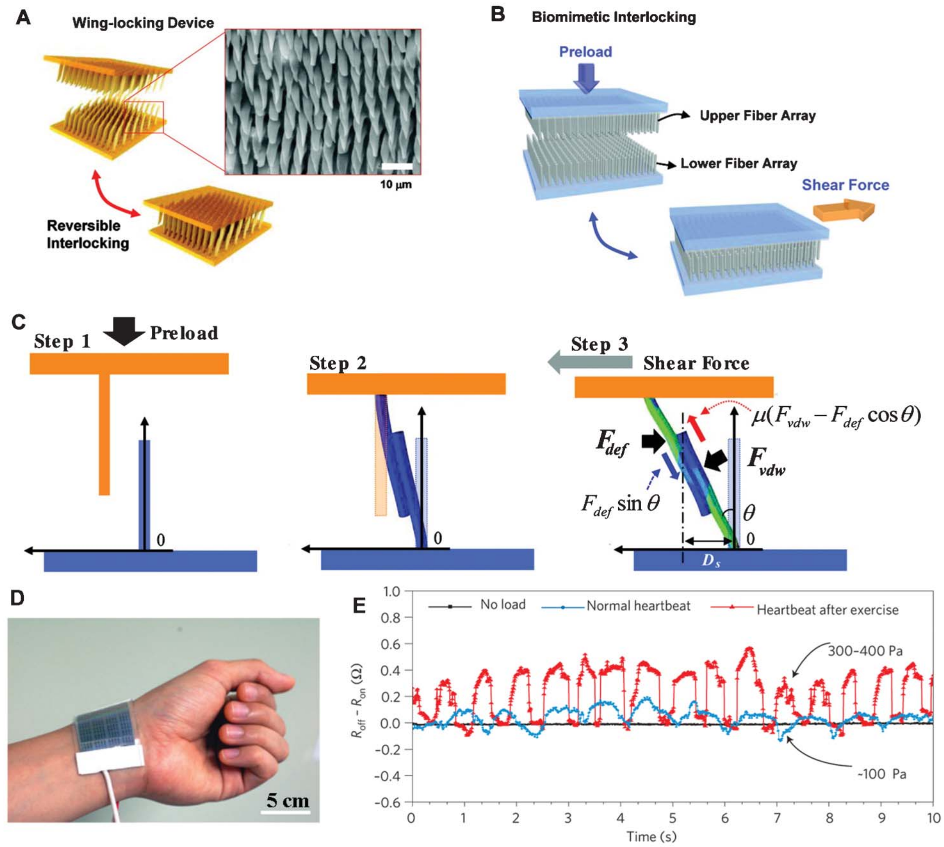

Fig. 11 (a) Schematic of folding and unfolding states of the wing-locking device of a beetle (*Promethis valgipes*) and SEM image of microtrichia on the cuticular surface. (b) Illustration of a beetle-inspired interlocking structure with upper and lower fiber arrays. (c) Sequences of interlocking steps: (Step 1) overlapping by a preload, (Step 2) paring of the fibers by VdW interactions, and (Step 3) distortion of the fibers upon application of an in-lane stretch in the shear direction.[76] (d) Photograph showing the skin-attachable sensor directly above the artery of the wrist and (e) measurement of the physical force of a heartbeat under normal ($\sim$60 beats min^{-1} with an average intensity of $\sim$100 Pa) and exercise conditions ($\sim$100 beats min^{-1} with an average intensity of 300–400 Pa).[78]

blueprints for artificial photonic materials.[7] Mimicking the cuticle of a beetle (*Plusiotis resplendens*), a new hetero-photonic band gap (PBG) structure has been developed which consists of an anisotropic nematic layer sandwiched between two cholesteric liquid-crystal layers with different helical pitches and, by doping the anisotropic defect layer with a laser dye, an efficient lasing was achieved.[59] The ultra-bright whiteness of certain beetle scales has inspired the development of optimization principles for the manufacture of white paper where it is normal to coat paper with nanoparticle scatterers, but typically the whiteness, and therefore the apparent "quality" of the paper, falls short of the whiteness in *Cyphochilus*.[50] Brilliant white fabric has also been produced using electrospun nanofiber webs.[123]

Inspired by the humidity change resulting in color changing behavior in longhorn beetles, an artificial humidity-sensitive colloidal PC was fabricated by infiltration of a hydrophilic polyacrylamide (PAAm) solution into the interstice of the opal template and subsequent photopolymerization.[105] The color of the PAAm–P(St–MMA–AA) PC hydrogel was sensitive to humidity; it could reversibly vary from transparent to violet, blue, cyan, green and red under various humidity conditions, covering the whole visible range (Fig. 10a and 10b). The strategy of structural color change may not only help obtain insight into the biological functionality of structural coloration, but may also inspire the design of novel artificial optical devices.[115] Inspired by the humidity-dependent color change observed in the cuticle of the Hercules beetle, a biomimetic thin-film-type humidity sensor with nanoporous structures (three-dimensional photonic crystals) was designed.[64] The visible color of the fabricated humidity sensor changed from blue-green to red as the environmental humidity increased.

A reversible interlocking was inspired by the wing-locking device of a beetle (*Promethis valgipes*) where densely populated microhairs (termed microtrichia) on the cuticular surface form numerous hair-to-hair contacts to maximize lateral shear adhesion.[76,77] Regularly arrayed microfibers are interconnected when the upper and lower layers are brought in contact, which in turn generates a high shear locking force against an in-plane stretch (Fig. 11a). Inspired by this wing-locking device, artificial micro- and nanofiber arrays were prepared as shown in Fig. 11b. The schematic in Fig. 11c shows the sequence of the interlocking steps: (Step 1) overlapping by a preload, (Step 2) pairing of the fibers by VdW interactions, and (Step 3) distortion of the fibers upon application of an in-plane stretch in the shear direction. Based on this reversible interlocking of nanofibers, a flexible and highly sensitive strain-gauge sensor was designed (Fig. 11d[78]).

When different sensing stimuli are applied, the degree of interconnection and the electrical resistance of the sensor changes in a reversible, directional manner with specific, discernible strain-gauge factors. The sensor can be used to monitor signals ranging from human heartbeats to the impact of a bouncing water droplet on a superhydrophobic surface. As shown in Fig. 11d and 11e, heartbeats under two different conditions, normal ($\sim$60 beats min^{-1} with an average intensity of $\sim$100 Pa) and post-exercise ($\sim$100 beats min^{-1} with an average intensity of 300–400 Pa), were monitored with time, suggesting that the signals could be differentiated by the discernible magnitudes and frequencies of the corresponding biofeedback (heartbeat).

In keeping with the high interest in MAVs, microfabrication technologies have been developed in an attempt to mimick a beetle wing to construct a realistic vein–membrane structure.[65] The folding/unfolding mechanisms of beetle hind wings may provide insight for portable MAVs with morphing wings.[3] By actuation of shape memory alloy wires, the artificial wings can be unfolded to provide an actuation force at the wing base and along the leading edge vein.[70] Also, wing folding/unfolding behavior provides inspiration to design biomimetic deployable systems.[48]

6. Summary

Since beetle wings exhibit special functionalities, they may help in developing new bioinspired designs in the fields of materials science and technology.

Elytra, as natural biocomposites optimized by nature over many centuries, have excellent mechanical and physical properties, such as light weight, high strength, superhydrophobic characteristics, color changes and anti-adhesion. Those are closely related to the microstructures both on the surface and on the inside. The wax filaments, scales arrays and grating microstructures will affect color changing. Their inner structure consisting of trabeculae, chitin fibers arrangement, helicoidal plies and preformed holes provides light mass and high strength which provides inspiration for the design of advanced composite materials. Biomimetic patterned films, fog-catching devices and appliances to clear fog from airport runways and improve dehumidification equipment have been developed by mimicking the *Stenocara* beetle gathering water from fog.

The wing locking system of elytra and folding/unfolding characteristics of hind wings are special features of beetles. They may provide insight for portable MAVs with morphing wings and give inspiration for the design of biomimetic deployable systems.

The mechanical properties of insect cuticle may provide guidelines for designing advanced composites. Based on tensile testing, the oriented arrangements of anisotropic fibres affect the mechanical properties of elytra. Since elytra are highly structured biological composite materials, it is difficult to measure their local mechanical properties. The nanoindenter enables investigation of the mechanical properties of beetle wings in detail, which assists in the optimization of biocomposites, and reveals their potential utility in materials science and engineering applications.

The study of the structure, functional and mechanical properties of beetle wings gives an opportunity to understand their behavior and characteristics. This can form a good basis for the research and development of bioinspired materials, structures, and smart devices.

Acknowledgements

This work was supported by the National Natural Science Foundation of China (grant no. 31172144), by the Science & Technology Development Projects of Jilin Province (grant no. 20090147), by the Basic Operation Foundation of Jilin University (grant no. 201200007), by the Project of the National Twelfth-Five Year Research Program of China (2011BAD20B09-15), and by "Project 985" of Jilin University.

References

1 E. Adachi, Unexpected variability of millennium green: structural color of Japanese jewel beetle resulted from thermosensitive porous organic multilayer, *J. Morphol.*, 2007, **268**, 826–829.
2 A. Balmert, B. H. Florian, P. Ditsche-Kuru and W. Barthlott, Dry under water: comparative morphology and functional aspects of air-retaining insect surfaces, *J. Morphol.*, 2011, **272**, 442–451.
3 P. R. Bhayu, Q. V. Nguyen, H. C. Park, N. S. Goo and D. Byun, Artificial cambered-wing for a beetle-mimicking flapper, *J. Bionic Eng.*, 2010, **7**, S130–S136.
4 B. Bhushan, Biomimetics: Lessons from Nature – An Overview, *Philos. Trans. R. Soc. London, Ser. A*, 2009, **367**, 1445–1486.
5 B. Bhushan, *Springer Handbook of Nanotechnology*, third edn, Springer-Verlag, Heidelberg, Germany, 2010.
6 B. Bhushan, *Biomimetics: Bioinspired Hierarchical-Structured Surfaces for Green Science and Technology*, Springer-Verlag, Heidelberg, Germany, 2012.
7 L. P. Biró, K. Kertész, E. Horváth, G. I. Márk, G. Molnár, Z. Vértesy, J.-F. Tsai, A. Kun, Zs. Bálint and J. P. Vigneron, Bioinspired artificial photonic nanoarchitecture using the elytron of the beetle *Trigonophorus rothschildi varians* as a 'blueprint', *J. R. Soc. Interface*, 2010, **7**, 887–894.
8 P. Bouchard and S. N. Gorb, The elytra-to-body binding mechanism of the flightless rainforest species *Tabarus montanus* Kaszab (Coleoptera: Tenebrionidea), *Arthropod Struct. Dev.*, 2000, **29**, 323–331.
9 J. H. Brackenbury, Wing folding in beetles, *In IUTAM-IASS Symposium on Deployable Structures: Theory and Applications*, edited by Pellegrino, S. and Guest, S. D., Kluwer Academic Publishers, Netherlands, 1998.
10 D. Byun, J. Hong, J. H. Ko Saputra, Y. J. Lee, H. C. Park, B. K. Byun and J. R. Lukes, Wetting characteristics of insect wing surfaces, *J. Bionic Eng.*, 2009, **6**, 63–70.
11 R. F. Chapman, *The Insects: Structure and function*, Cambridge, New York, 1998.
12 B. Chen, X. Peng, W. Wang, J. Zhang and R. Zhang, Research on the microstructure of insect cuticle and the strength of a biomimetic preformed hole composite, *Micron*, 2002, **33**, 571–574.
13 J. X. Chen, Q. Q. Ni, Y. L. Xua and M. Iwamotoc, A biomimetic approach for creating thermally stable polyimide-coated honeycomb films, *Compos. Struct.*, 2007, **79**, 331–337.
14 J. X. Chen, G. Z. Dai, Y. L. Xu and M. Iwamoto, Optimal composite structures in the forewings of beetles, *Compos. Struct.*, 2007, **81**, 432–437.
15 J. X. Chen, J. Xie, H. Zhu, S. J. Guan, G. Wu, M. N. Noori and S. J. Guo, Integrated honeycomb structure of a beetle forewing and its imitation, *Mater. Sci. Eng., C*, 2012, **32**, 613–618.
16 H. Cheng, M. S. Chen and J. R. Sun, Histological structures of the dung beetle, *Copris ochus* Motschulsky integument, *Acta Entomologica Sinica*, 2003, **46**, 429–435.
17 J. H. Choi, Y. M. Kim, Y. W. Park, T. H. Park, K. Y. Dong and B. K. Ju, Hydrophilic dots on hydrophobic nanopatterned surfaces as a flexible gas barrier, *Langmuir*, 2009, **25**, 7156–7160.

18 J. Cracraft and M. J. Donoghue, *Assembling the Tree of Life*, Oxford University Press, New York2002.
19 Z. D. Dai and Z. X. Yang, Macro-/micro-structures of elytra, mechanical properties of the biomaterial and the coupling strength between elytra in beetles, *J. Bionic Eng.*, 2010, **7**, 6–12.
20 C. Dorrer and J. Rühe, Mimicking the stenocara beetles dewetting of drops from a patterned superhydrophobic surface, *Langmuir*, 2008, **24**, 6154–6158.
21 C. Eichler, J. Lomakin, Y. Arakane, K.J. Kramer, M.R. Kanost, S. H. Gehrke and R.W. Beeman, Insect cuticle as a biomimetic material, in *Proceedings of American Institute of Chemical Engineers Annual Meeting*, 2006, pp. 4309–4313, edited by A. Peppas and J. Z. Hilt, Cincinnati, OH.
22 S. Enders, N. Barbakadse, S. N. Gorb and E. Arzt, Exploring biological surfaces by nanoindentation, *J. Mater. Res.*, 2004, **19**, 880–887.
23 J. H. Fan, B. Chen, Z. H. Gao and C. T. Xiang, Mechanisms in failure prevention of bio-materials and bio-structures, *Mech. Adv. Mater. Struct.*, 2005, **12**, 229–237.
24 T. X. Fan, S. K. Chow and D. Zhang, Biomorphic mineralization: From biology to materials, *Prog. Mater. Sci.*, 2009, **54**, 542–659.
25 D. N. Fedorenko, Evolution of the Beetle Hind Wing, With Special Reference to Folding (Insecta, Coleoptera), Pensoft Publishers, Bulgaria, 2009.
26 J. G. Fernandez and D. E. Ingber, Unexpected strength and toughness in chitosan-fibroin laminates inspired by insect cuticle, *Adv. Mater.*, 2012, **24**, 480–484.
27 R. G. Foottit and P. H. Adler, Insect Biodiversity: Science and Society, Blackwell Publishing, West Sussex, UK, 2009.
28 W. T. M. Forbes, How a beetle folds its wings, *Psyche*, 1924, **31**, 254–258.
29 L. Frantsevich, Mechanisms modeling the double rotation of the elytra in beetles (Coleoptera), *J. Bionic Eng.*, 2011, **8**, 395–405.
30 L. Frantsevich, Double rotation of the opening (closing) elytra in beetles (Coleoptera), *J. Insect Physiol.*, 2012, **58**, 24–34.
31 J. W. Galusha, L. R. Richey, J. S. Gardner, J. N. Cha and M. H. Bartl, Discovery of a diamond-based photonic crystal structure in beetle scales, *Phys. Rev. E: Stat., Nonlinear, Soft Matter Phys.*, 2008, **77**, 050904–050907.
32 J. W. Galusha, M. R. Jorgensen and M. H. Bartl, Diamond-structured titania photonic-bandgap crystals from biological templates, *Adv. Mater.*, 2010, **27**, 107–110.
33 J. W. Galusha, L. R. Richey, M. R. Jorgensen, J. S. Gardner and M. H. Bartl, Study of natural photonic crystals in beetle scales and their conversion into inorganic structures via a sol–gel bio-templating route, *J. Mater. Chem.*, 2010, **20**, 1277–1284.
34 R. P. Garrod, L. G. Harris, W. C. Schofield, J. McGettrick, L. J. Ward, D. O. Teare and J. P. Badyal, Mimicking a stenocara beetle's back for microcondensation using plasmachemical patterned superhydrophobic-superhydrophilic surfaces, *Langmuir*, 2007, **23**, 689–693.
35 S. N. Gorb, Frictional surfaces of the elytra-to-body arresting mechanism in tenebrionid beetles (Coleoptera–Tenebrionidae) – design of co-opted fields of microtrichia and cuticle, *Int. J. Insect Morphol. Embryol.*, 1998, **27**, 205–225.
36 S. N. Gorb, Ultrastructure of the thoracic dorso-medial field (TDM) in the elytra-to-body arresting mechanism in Tenebrionid Beetles (Coleoptera: Tenebrionidae), *J. Morphol.*, 1999, **240**, 101–113.
37 S. N. Gorb, Attachment devices of insect cuticle, Kluwer Academic Publishers, Netherlands, 2001.
38 S. N. Gorb, Insect-Inspired Technologies: Insects as a Source for Biomimetics, In *Insect Biotechnology, (Biologically-Inspired Systems)*, edited by Vilcinskas, Giessen, Germany, 2011.
39 D. A. Grimaldi and M. S. Engel, Evolution of the Insects, Cambridge University Press, New York, 2005.
40 S. L. Gunderson and J. A. Lute, The use of preformed holes for increased strength and damage tolerance of advanced composites, *J. Reinf. Plast. Compos.*, 1993, **12**, 559–569.
41 S. L. Gunderson, R. G. Schiavone, Microstructure of an insect cuticle and applications to advanced composites, In *Biomimetics: Design and Processing of Materials*, edited by M. Sariksya and I. A. Aksay, American Institute of Physics, 1995.
42 N. S. Ha, T. L. Jin, N. S. Goo and H. C. Park, Anisotropy and non-homogeneity of an *Allomyrina Dichotoma* beetle hind wing membrane, *Bioinspir. Biomimetics*, 2011, **6**, 046003.
43 F. Haas, Geometry and mechanics of hind-wing folding in Dermaptera and Coleoptera. Master Thesis, University of Exeter, UK, 1994.
44 F. Haas and R. G. Beutel, Wing folding and the functional morphology of the wing base in Coleoptera, *Zoology*, 2001, **104**, 123–141.
45 F. Haas and R. J. Wootton, Two basic mechanisms in insect wing folding, *Proc. R. Soc. London, Ser. B*, 1996, **263**, 1651–1658.
46 F. Haas, S. Gorb and R. Blickhan, The function of resilin in beetle wings, *Proc. R. Soc. London, Ser. B*, 2000, **267**, 1375–1381.
47 F. Haas, S. Gorb and R. J. Wootton, Elastic joints in dermapteran hind wings: materials and wing folding, *Arthropod Struct. Dev.*, 2000, **29**, 137–146.
48 C. Hachem, E. Karni and A. Hanaor, Evaluation of biological deployable systems, *International Journal of Space Structures*, 2005, **20**, 189–200.
49 N. F. Hadley, Wax secretion and color phases of the desert tenebrionid beetle *Cryptoglossa verrucosa* (LeConte), *Science*, 1979, **203**, 367–369.
50 B. T. Hallam, A. G. Hiorns and P. Vukusic, Developing optical efficiency through optimized coating structure: biomimetic inspiration from white beetles, *Appl. Opt.*, 2009, **48**, 3243–3249.
51 P. M. Hammond, Wing-folding mechanism of beetles, with special reference to investigations of adephagan phylogeny (Coleoptera), in *Carabid beetles: Their evolution, natural history, and classification*, edited by T. Ervin and G. E. Ball, Smithsonian Institution, Washington, D.C., 1979.
52 P. M. Hammond, Dimorphism of wings, wing-folding and wing-toiletry devices in the ladybird, *Rhyzobius litura* (F.) (Coleoptera: Coccinellidae), with a discussion of inter-population variation in this and other wing-dimorphic beetle species, *Biol. J. Linn. Soc.*, 1985, **24**, 15–33.
53 G. Hangay and P. Zborowski, A Guide to the Beetles of Australia, CSIRO Publishing, Collingwood, Australia, 2010.
54 J. R. Henschel and M. K. Seely, Ecophysiology of atmospheric moisture in the Namib Desert, *Atmos. Res.*, 2008, **87**, 362–368.
55 H. R. Hepburn and A. Ball, On the structure and mechanical properties of beetle shells, *J. Mater. Sci.*, 1973, **8**, 618–623.
56 H. E. Hinton, Some structures of insects as seen with the scanning electron microscope, *Micron*, 1969, **1**, 84–108.
57 H. E. Hinton and G. M. Jarman, Physiological colour change in the elytra of the Hercules beetle, *Dynastes Hercules*, *J. Insect Physiol.*, 1973, **19**, 533–549.
58 M. W. Holdgate, The wetting of insect cuticle by water, *J. Exp. Biol.*, 1955, **32**, 591–617.
59 J. Hwang, M. H. Song, B. Park, S. Nishimura, T. Toyooka, J. W. Wu, Y. Takanishi, K. Ishikawa and H. Takezoe, Electro-tunable optical diode based on photonic band gap liquid-crystal heterojunctions, *Nat. Mater.*, 2005, **4**, 383–387.
60 M. Iwamoto, J. Chen, K. Kurashiki and Q. Q. Ni, Chitin fibre and its laminated structure of the fore-wing of beetle, In *High Performance Structures and Composites*, 2002, pp. 127–136, edited by C. A. Brebbia and W. P. de Wilde, WIT Press, Southampton, UK.
61 S. A. Jewell, P. Vukusic and N. W. Roberts, Circularly polarized colour reflection from helicoidal structures in the beetle *Plusiotis boucardi*, *New J. Phys.*, 2007, **9**, 99–1-10.
62 T. Jin, N. S. Goo, S. C. Woo and H. C. Park, Use of a digital image correlation technique for measuring the material properties of beetle wing, *J. Bionic Eng.*, 2009, **6**, 224–231.
63 P. Kejzlar, L. Voleský, Z. Andršová and D. Kroisov, Bionics and Nanotechnology, in *Proc. 3rd Inter. Conf. NANOCON'11* (Edited by R. R. Zbořil), 2011, pp. 174–179, Tanger Ltd., Brno, Czech Republic.
64 J. H. Kim, J.H. Moon, S. Y. Lee and J. Park, Biologically inspired humidity sensorbased on three-dimensional photonic crystals, *Appl. Phys. Lett.*, 2010, **97**, 103701.
65 J. H. Ko, J. Kim, J. Hong, Y. Yoo, Y. Lee, T. L. Jin, H. C. Park, N. S. Goo and D. Byun, Micro/nanofabrication for a realistic beetle wing with a superhydrophobic surface, *Bioinspir. Biomimetics*, 2012, **7**, 016011–1-8.
66 F. Liu, B. Q. Dong, X. H. Liu, Y. M. Zheng and J. Zi, Structural color change in longhorn beetles *Tmesisternus isabellae*, *Opt. Express*, 2009, **17**, 16183–16191.

67 J. Lomakin, P. A. Huber, C. Eichler, Y. Arakane, K. J. Kramer, R. W. Beeman, M. R. Kanost and S. H. Gehrke, Mechanical properties of the beetle elytron, a biological composite material, *Biomacromolecules*, 2011, **12**, 321–335.

68 S. M. Luke, B. T. Hallam and P. Vukusic, Structural optimization for broadband scattering in several ultra-thin white beetle scales, *Appl. Opt.*, 2010, **49**, 4246–4254.

69 C. W. Mason, Structural Colors in Insects. II, *J. Phys. Chem.*, 1927, **31**, 321–354.

70 A. Muhammad, H. C. Park, D. Y. Hwang, D. Byun and N. S. Goo, Mimicking unfolding motion of a beetle hind wing, *Chin. Sci. Bull.*, 2009, **54**, 2416–2424.

71 A. C. Neville, Biology of the Arthropod Cuticle. Springer, New York, 1975.

72 T. R. New, Beetles Conservation, Springer, Dordrecht, Netherlands, 2007.

73 Q. V. Nguyen, H. C. Park, N. S. Goo and D. Byun, Characteristics of a beetle's free flight and a flapping-wing system that mimics beetle flight, *J. Bionic Eng.*, 2010, **7**, 77–86.

74 J. Noble-Nesbitt, Structural aspects of penetration through insect cuticles, *Pestic. Sci.*, 1970, **1**, 204–208.

75 H. Onslow, On a periodic structure in many insect scales, and the cause of their iridescent colours, *Philos. Trans. R. Soc. London, Ser. B*, 1923, **211**, 1–74.

76 C. Pang, D. Kang, T. Kim and K. Y. Suh, Analysis of preload-dependent reversible mechanical interlocking using beetle-inspired wing locking device, *Langmuir*, 2012, **28**, 2181–2186.

77 C. Pang, T. I. Kim, W. G. Bae, D. Kang, S. M. Kim and K. Y. Suh, Bioinspired reversible interlocker using regularly arrayed high aspect-ratio polymer fibers, *Adv. Mater.*, 2012, **24**, 475–479.

78 C. Pang, G.Y. Lee, T. I. Kim, S. M. Kim, H. N. Kim, S. H. Ahn and K. Y. Suh, A flexible and highly sensitive strain-gauge sensor using reversible interlocking of nanofibres, *Nat. Mater.*, 2012, **11**, 795–801.

79 G. J. Parker, Biomimetically-inspired photonic nanomaterials, *J. Mater. Sci.: Mater. Electron.*, 2010, **21**, 965–979.

80 A. R. Parker and C. R. Lawrence, Water capture by a desert beetle, *Nature*, 2001, **414**, 33–34.

81 A. R. Parker, D. R. McKenzie and M. C. J. Large, Multilayer reflectors in animals using green and gold beetles as contrasting examples, *J. Exp. Biol.*, 1998, **201**, 1307–1313.

82 A. Parker, V. L. Welch, D. Driver and N. Martini, Structural colour: opal analogue discovered in a weevil, *Nature*, 2003, **426**, 786–787.

83 D. P. Pulsifer and A. Lakhtakia, Background and survey of bioreplication techniques, *Bioinspir. Biomimetics*, 2011, **6**, 031001–1-11.

84 D. Quéré, Non-sticking drops, *Rep. Prog. Phys.*, 2005, **68**, 2495–2532.

85 M. Rassart, J. F. Colomer, T. Tabarrant and J. P. Vigneron, Diffractive hygrochromic effect in the cuticle of the hercules beetle *Dynastes hercules*, *New J. Phys.*, 2008, **10**, 033014–1-14.

86 M. Rassart, P. Simonis, A. Bay, O. Deparis and J. P. Vigneron, Scale coloration change following water absorption in the beetle *Hoplia coerulea* (Coleoptera), *Phys. Rev. E: Stat., Nonlinear, Soft Matter Phys.*, 2009, **80**, 031910–1-6.

87 L. Q. Ren, J. Tong, J. Q. Li and B. C. Chen, Soil adhesion and biomimetics of soil-engaging components: a review, *J. Agric. Eng. Res.*, 2001, **79**, 239–263.

88 G. H. Rosado-Neto and G. Santos, B. Dos, The elytro-tergal stridulatory apparatus of the genus *Bondarius* Rosado-Neto (Coleoptera, Curculionidae), *Rev. Bras. Entomol.*, 2010, **54**, 337–338.

89 G.A. Samuelson, An elytron to body meshing mechanism of possible significance in the higher classification of Chrysomelidae (Coleoptera), In *Proceedings of the Third International Symposium on the Chrysomelidae*, Backhuys Publishers, Leiden, Netherlands, 1994, pp. 136–147.

90 G.A. Samuelson, Binding sites: elytron-to-body meshing structures of possible significance in the higher classification of Chrysomeloidea, in *Chrysomelidae Biology, The Classification, Phylogeny and Genetics*, edited by Jolivet, P. H. A. and Cox, M. L., SPB Academic Publishing, Amsterdam, Netherlands, 1996, pp. 267–290.

91 T. D. Schowalter, Insect Ecology: An Ecosystem Approach, second edition, Elsevier, London, UK, 2009.

92 T. D. Schultz and G. D. Bernard, Pointillistic mixing of interference colours in cryptic tiger beetles, *Nature*, 1989, **337**, 72–73.

93 A. E. Seago, P. Brady, J. P. Vigneron and T. D. Schultz, Gold bugs and beyond: a review of iridescence and structural colour mechanisms in beetles (Coleoptera), *J. R. Soc. Interface*, 2009, **6**, S165–S184.

94 V. Sharma, M. Crne, J. O. Park and M. Srinivasarao, Structural origin of circularly polarized iridescence in jeweled beetles, *Science*, 2009, **325**, 449–451.

95 N. J. Shirtcliffe, G. McHale and M. I. Newton, The super-hydrophobicity of polymer surfaces: recent developments, *J. Polym. Sci., Part B: Polym. Phys.*, 2011, **49**, 1203–1217.

96 M. Shimomura, The new trends in next generation biomimetics material technology: learning from biodiversity, *Q. Rev.*, 2010, **37**, 53–75.

97 L. D. Silva, I. Hodgkinson, P. Murray, Q. H. Wu, M. Arnold, J. Leader and A. Mcnaughton, Natural and nanoengineered chiral reflectors: structural color of Manuka beetles and titania coatings, *Electromagnetics*, 2005, **25**, 391–408.

98 M. Srinivasarao, Nano-optics in the biological world: Beetles, butterflies, birds, and moths, *Chem. Rev.*, 1999, **99**, 1935–1961.

99 J. Sun and B. Bhushan, The structure and mechanical properties of dragonfly wings and their role on flyability, *C. R. Mecan., Fr. Acad. .Sci.*, 2012, **340**, 3–17.

100 J. Y. Sun and J. Tong, Fracture toughness properties of three different biomaterials measured by nanoindentation, *J. Bionic Eng.*, 2007, **4**, 11–17.

101 J.Y. Sun, J. Tong, D. H. Chen, J. B. Lin, X. P. Liu and Y. M. Wang, Micro-tensile testing of the lightweight laminated structures of beetle elytra cuticle, *Adv. Natur. Sci.*, 2010, **3**, 225–234.

102 J. Y. Sun, X. P. Liu, J. Tong and Z. Y. Yue, Sensitive elastic modulus mapping of micro-structured biomaterials, *Sixth International Symposium on Precision Engineering Measurements and Instrumentation*, edited by Jiubin Tan, Xianfang Wen, Proc. of SPIE2010b, **Vol. 7544**, 754448-1-10.

103 J. Y. Sun, J. Tong and Z. J. Zhang, Nanomechanical properties and the hierarchical structure of elytra cuticle of dung beetle (*Copris ochus* Motschulsky), *The 2009 : IEEE International Conference on Mechatronics and Automation (ICMA 2009)*, 2009, 4277–4282.

104 J. Y. Sun, J. Tong and J. Zhou, Application of nano-indenter for investigation of the properties of the elytra cuticle of the dung beetle (*Copris ochus* Motschulsky), *IEE Proc.: Nanobiotechnol.*, 2006, **153**, 129–133.

105 E. T. Tian, J. X. Wang, Y. M. Zheng, Y. L. Song, L. Jiang and D. B. Zhu, Colorful humidity sensitive photonic crystal hydrogel, *J. Mater. Chem.*, 2008, **18**, 1116–1122.

106 J. Tong, J. Y. Sun, D. H. Chen and S. Zhang, Geometrical features and wettability of dung beetles and potential biomimetic engineering applications in tillage implements, *Soil Tillage Res.*, 2005, **80**, 1–12.

107 J. Tong, B. Moayad, Y. H. Ma, J. Y. Sun, D. H. Chen, H. L. Jia and L. Q. Ren, Effects of biomimetic surface designs on furrow opener performance, *J. Bionic Eng.*, 2009, **63**, 280–289.

108 J. Tong, M. Mohammad, J. Zhang, Y. H. Ma, B. J. Rong, D. H. Chen and C. Menon, DEM numerical simulation of abrasive wear characteristics of a bioinspired ridged surface, *J. Bionic Eng.*, 2010, **7**, 175–181.

109 J. P. Vigneron, J. M. Pasteels, D. M. Windsor, Z. Vértesy, M. Rassart, T. Seldrum, J. Dumont, O. Deparis, V. Lousse, L. P. Biró, D. Ertz and V. Welch, Switchable reflector in the Panamanian tortoise beetle *Charidotella egregia* (Chrysomelidae: Cassidinae), *Phys. Rev. E: Stat., Nonlinear, Soft Matter Phys.*, 2007, **76**, 031907–1-10.

110 A. P. Vogler and K. C. Kelley, Covariation of defensive traits in tiger beetles (Genus *Cicindela*): A phylogenetic approach using mtDNA, *Evolution*, 1998, **52**, 529–538.

111 D. Voigt, H. Peisker and S. Gorb, Visualization of Epicuticular Grease on the Covering Wings in the Colorado Potato Beetle: A Scanning Probe Approach, in *Applied Scanning Probe Methods XIII*, edited by B. Bhushan and H. Fuchs, Springer Berlin Heidelberg, Germany, 2009, pp.1–16.

112 P. Vukusic, B. Hallam and J. Noyes, Brilliant whiteness in ultrathin beetle scales, *Science*, 2007, **315**, 348–349.

113 V. Welch and J. Vigneron, Beyond butterflies- the diversity of biological photonic crystals, *Opt. Quantum Electron.*, 2007, **39**, 295–303.
114 V. Welch, V. Lousse, O. Deparis, A. Parker and J. Vigneron, Orange reflection from a three-dimensional photonic crystal in the scales of the weevil *Pachyrrhynchus congestus pavonius* (Curculionidae), *Phys. Rev.*, 2007, **E75**, 41919–1-9.
115 J. X. Wang, Y. Z. Zhang, S. T. Wang, Y. L. Song and L. Jiang, Bioinspired Colloidal Photonic Crystals with Controllable Wettability, *Acc. Chem. Res.*, 2011, **44**, 405–415.
116 T. Wagner, C. Neinhuis and W. Barthlott, Wettability and contaminability of insect wings as a function of their surface sculptures, *Acta Zool.*, 1996, **77**, 213–225.
117 R. J. Wootton, Support and deformability in insect wings, *J. Zool.*, 1981, **193**, 447–468.
118 R. J. Wootton, Functional morphology of insect wings, *Annu. Rev. Entomol.*, 1992, **37**, 113–140.
119 R. J. Wootton, Invertebrate paraxial locomotory appendages: design, deformation and control, *J. Exp. Biol.*, 1999, **202**, 3333–3345.
120 H. A. B. Wösten, T. G. Ruardy, H. C. van der Mei, H. J. Busscher and J. G. H. Wessels, Interfacial self-assembly of a *Schizophyllum commune* hydrophobin into an insoluble amphipathic protein membrane depends on surface hydrophobicity, *Colloids Surf., B*, 1995, **5**, 189–195.
121 H. Yabu, Y. Nakamichi, Y. Hirai and M. Shimomura, A biomimetic approach for creating thermally stable polyimide-coated honeycomb films, *Chem. Lett.*, 2011, **40**, 597–599.
122 Y. L. Yang, C. C. Hsu, T. L. Chang, L. S. Kuo and P. H. Chen, Study on wetting properties of periodical nanopatterns by a combinative technique of photolithography and laser interference lithography, *Appl. Surf. Sci.*, 2010, **256**, 3683–3687.
123 J. Yip, S.P. Ng and K. H. Wong, Brilliant whiteness surfaces from electrospun nanofiber webs, *Text. Res. J.*, 2009, **79**, 771–779.
124 M. P. Zari, Biomimetic approaches to architectural design for increased sustainability, School of architecture, Victoria University, NZ, 2007.
125 L. Zhai, M. C. Berg, F. C. Cebeci, Y. Kim, J. M. Milwid, M. F. Rubner and R. E. Cohen, Patterned superhydrophobic surfaces: Toward a synthetic mimic of the namib desert beetle, *Nano Lett.*, 2006, **6**, 1213–1217.